

SULFONATED STYRENE-CO-MALEIC ACID AND ITS DERIVATIVES AS
SUPERLASTICIZERS IN CONCRETE

A THESIS SUBMITTED TO
THE GRADUATE SCHOOL OF NATURAL AND APPLIED SCIENCES
OF
MIDDLE EAST TECHNICAL UNIVERSITY

BY
SEÇİL YENİAY

IN PARTIAL FULFILLMENT OF THE REQUIREMENTS
FOR
THE DEGREE OF MASTER OF SCIENCE
IN
CHEMISTRY

APRIL 2008

Approval of the thesis:

**SULFONATED STYRENE-CO-MALEIC ACID AND ITS DERIVATIVES AS
SUPERLASTICIZERS IN CONCRETE**

submitted by **SEÇİL YENİAY** in partial fulfillment of the requirements for the
degree of **Master of Science in Chemistry Department, Middle East
Technical University** by,

Prof. Dr. Canan Özgen
Dean, Graduate School of **Natural and Applied Sciences**

Prof. Dr. Ahmet Önal
Head of Department, **Chemistry**

Prof. Dr. Leyla Aras
Supervisor, **Chemistry Dept., METU**

Examining Committee Members:

Prof. Dr. Duygu Kısakürek
Chemistry Dept., METU

Prof. Dr. Leyla Aras
Chemistry Dept., METU

Prof. Dr. Zuhale Küçükayavuz
Chemistry Dept., METU

Prof. Dr. Ali Güner
Chemistry Dept., Hacettepe University

Asst. Prof. Dr. Erdal Onurhan
METU-Northern Cyprus Campus

Date:

I hereby declare that all information in this document has been obtained and presented in accordance with academic rules and ethical conduct. I also declare that, as required by these rules and conduct, I have fully cited and referenced all material and results that are not original to this work.

Name, Last name : Seil Yeniay

Signature :

ABSTRACT

SULFONATED STYRENE-CO-MALEIC ACID AND ITS DERIVATIVES AS SUPERPLASTICIZERS IN CONCRETE

Yeniay, Seil

M.Sc., Department of Chemistry

Supervisor: Prof. Dr.Leyla Aras

April 2008, 71 pages

In the past three decades, a new group of concrete admixtures, termed “superplasticizers”, were introduced to the concrete industry. They have gained wide acceptance because of their many advantages. The addition of superplasticizers to concrete improves the workability and strength of concrete. In this study, the effect of the chemical structure of poly (4-styrenesulfonic acid-co-maleic acid) sodium salt (SSAMA), which contains both sulfonic and carboxylic acid groups, which is a new superplasticizer, was analyzed. Two different molecular weights of PEG (polyethylene glycol monomethyl ether) were grafted to this water-soluble copolymer at different weight compositions. The structures of synthesized copolymers were verified by FTIR and NMR analyses. The molecular weight difference of the grafted copolymers with different side chain lengths was determined by dilute solution viscosimetry. The effects of chemical structure of grafted copolymers on the fluidity of cement paste and the mechanical properties of the mortars

were investigated. The zeta potential measurements revealed the interactions between the cement particles and polycarboxylate type superplasticizers.

The maximum fluidity was achieved for the PEG grafted copolymer with the weight ratio 3:3. The mechanical properties of this copolymer showed the highest flexural and compressive strength compared to other copolymers.

The addition of various Li salts to SSAMA affected the ionic medium, therefore, the dispersion performance of cement paste and the mechanical properties of the mortars improved. The mixture of LiCl: SSAMA in 1:1 mol ratio exhibited the maximum fluidity compared to other Li salts and their compositions. This mixture gave the highest flexural strength but the mixture of Li_2CO_3 in 1:1 composition gave the highest compressive strength in each salt mixtures.

Keywords: Superplasticizers, Polycarboxylates, Poly(4-styrenesulfonic acid-co-maleic acid)sodium salt, Fluidity, Zeta Potential

ÖZ

BETONDA SÜPERAKIŞKANLAŞTIRICI OLARAK SÜLFONLANMIŞ STİREN-CO-MALEİK ASİT VE TÜREVLERİNİN KULLANIMI

Yeniay, Seçil

Yüksek Lisans, Kimya Bölümü

Tez Yöneticisi: Prof. Dr. Leyla Aras

Nisan 2008, 71 sayfa

Geçen 30 yılda, süperakışkanlaştırıcı adı verilen, yeni bir grup olan katkı maddeleri beton endüstrisine sunuldu. Birçok avantajları olması nedeniyle yaygın kabul gördü. Betona süperakışkanlaştırıcıların katkısı betonun işlenebilirliğini ve mukavemetini artırır. Bu çalışmada, yeni bir süperakışkanlaştırıcı olan sülfonik ve karboksilik asit grupları içeren poli(4-stirensülfonik asit-maleik asit)sodyum tuzunun kimyasal yapısının etkisi analiz edildi. Bu suda çözünebilen kopolimere farklı ağırlık kompozisyonlarında, iki farklı moleküler ağırlıkta olan PEG (polietilen glikol monometil eter) aşılandı. Sentezlenen kopolimerlerin yapıları FTIR ve NMR analizleri ile doğrulandı. Farklı yan zincir uzunlukları olan aşılanmış kopolimerlerin molekül ağırlık farklılığı seyreltik solüsyon viskozitesi ile saptandı. Aşılanmış kopolimerlerin kimyasal yapısının çimento pastasının akışkanlığına etkileri ve betonun mekanik özellikleri araştırıldı. Zeta potansiyel ölçümleri çimento parçacıkları ile polikarboksilik tip süperakışkanlaştırıcıların etkileşimlerini açığa çıkardı. Maksimum yayılma,

3:3 ağırlık oranında PEG aşılınmış kopolimer için sağlandı. Bu kopolimerin mekanik özellikleri diğer kopolimerlere göre en yüksek bükülme ve basınç mukavemeti gösterdi.

Çeşitli Li tuzlarının SSAMA ya katkısı iyonik ortamı etkiledi ve böylece çimento pastasının yayılma performansı ve betonun mekanik özellikleri gelişti. 1:1 mol oranında LiCl: SSAMA karışımı diğer Li tuzlarına ve kompozisyonlarına göre maksimum yayılma gösterdi. Bu karışım en yüksek bükülme mukavemeti verdi fakat Li_2CO_3 ın 1:1 kompozisyonu diğer tuz karışımları içinde en yüksek basınç mukavemeti verdi.

Anahtar kelimeler: Süperakışkanlaştırıcılar, Polikarboksilikler, Poli(4-stirensülfonik asit-co-maleik asit)sodyum tuzu, Yayılma, Zeta Potansiyel

To my family...

ACKNOWLEDGEMENTS

I would like to express my most sincere gratitude to my supervisor Prof. Dr. Leyla ARAS for her valuable guidance, kind helps and encouragement throughout this thesis.

I am greatly indebted Arzu Büyükyavaş, Gözde Tuzcu and Tuba Ecevit for their endless helps, inspirations and wonderful advices in building up my thesis.

I would like to express my special thanks to Ali Sinan Dike for relieving my mind throughout my thesis and for his helpful personality and friendship. I would also thank Güralp Özkoç for his excellent cooperation.

My sincere appreciation also goes to Civil Engineering Department staff of METU. I would like to thank Asist. Prof. Dr. İsmail Özgür Yaman for his support and interest and I would like to thank Cuma Yıldırım and Ali Sümbüle for their kind helps and collaborations during the mechanical tests.

I would like to dedicate this thesis to Volkan Yeniay for his valuable love and support. He always helped me to get through all the obstacles in my life. I would also like to thank his family for their helps during writing my thesis.

Finally, I would like to thank my parents and my brother Ali Selçuk Yeniay, for their never ending helps, encouragement and love. I will not be able to complete my work without their support.

TABLE OF CONTENTS

ABSTRACT	iv
ÖZ	vi
ACKNOWLEDGEMENTS	ix
TABLE OF CONTENTS	x
LIST OF TABLES	xiv
LIST OF FIGURES	xv
LIST OF ABBREVIATIONS	xvii
CHAPTER	
1.INTRODUCTION	1
1.1. Concrete	1
1.1.1. Cement	2
1.1.2. Water	3
1.1.3. Aggregates	4
1.1.4. Additives	5
1.2. Superplasticizers	8
1.2.1. Effects of Superplasticizers	9
1.2.2. Types of Superplasticizers	12
1.2.2.1. Lignosulphonates	14
1.2.2.2. Sulphonated Naphthalene Formaldehyde	15
1.2.2.3. Sulphonated Melamine Formaldehyde	15
1.2.2.4. Polycarboxylates	16
1.2.3. Applications of Superplasticizers	20
1.3. Concrete Properties	20
1.3.1. Workability	20
1.3.2. Setting	22
1.3.3. Bleeding and Segregation	22
1.3.4. Mechanical Properties	23

1.4. Aim of the Study.....	24
2.EXPERIMENTAL	25
2.1. Chemicals.....	25
2.2. Instrumentation.....	25
2.2.1. Fourier Transform Infrared Spectroscopy	25
2.2.2. Nuclear Magnetic Resonance (NMR)	26
2.2.3. Dilute Solution Viscosimetry	26
2.2.4. Zeta Potential.....	26
2.2.5. Mini Slump Test	30
2.2.6. Mechanical Measurements of Mortars Prepared with Polymer Samples.....	31
2.2.6.1. <i>Flexural Strength Measurements</i>	31
2.2.6.2. <i>Compressive Strength Measurements</i>	33
2.3. Synthesis.....	35
2.3.1. Synthesis of Poly (ethylene glycol) monomethyl ether-g-poly(4- styrenesulfonic acid-co-maleic acid)sodium salt (SSAMA-g-PEG)	35
2.3.2. Adding Different Li ⁺ Salts into the Medium.....	37
3.RESULTS AND DISCUSSION.....	38
3.1. Characterization of the Polymers	38
3.1.1. FTIR Results.....	38
3.1.2. NMR Results.....	42
3.1.2.1. ¹ H NMR and ¹³ C NMR Characterization of SSAMA	42
3.1.2.2. ¹ H and ¹³ C NMR Characterization of A33.....	43
3.1.2.3. ¹ H and ¹³ C NMR Characterization of B55.....	45
3.2. Dilute Solution Viscosity Results	46
3.2.1. Dilute Solution Viscosity of SSAMA	46
3.2.2. Dilute Solution Viscosity of A32 and A41	47
3.2.3. Dilute Solution Viscosity of B64 and B82	48
3.3. Zeta Potential Results	49
3.4. Mini Slump Test.....	52
3.4.1. Mini Slump Test Results for PEG2000 Grafted SSAMA	52
3.4.2. Mini Slump Test Results for PEG1100 Grafted SSAMA	53

3.4.3. Mini Slump Test Results for Li salts of SSAMA	55
3.5. Mechanical Strength Test Results.....	57
3.5.1. Flexural Strength Test Results.....	57
3.5.2. Compressive Strength Test Results.....	59
4.CONCLUSION	62
REFERENCES	64
APPENDIX A. FTIR SPECTRA OF THE GRAFTED COPOLYMERS	68

LIST OF TABLES

TABLES

Table 1.2 Composition of Portland cement with chemical composition and weight percent.....	3
Table 1.3 Classes of Aggregates	5
Table 1.4 A table of admixtures and their functions	8
Table 2.1 The composition ratios of monomers used in the preparation of PEG grafted copolymers	36
Table 2.2 Schematic representation of the mixture of Li salts and SSAMA .	36
Table 3.1 Maximum flexural stresses experienced by the mortar samples..	58
Table 3.2 Flexural strenghts of the mortar samples	59
Table 3.3 Maximum compressive stresses experienced by the mortar samples	60
Table 3.4 Compressive strengths of the mortar samples	60

LIST OF FIGURES

FIGURES

Figure 1.1 The composition of concrete.....	2
Figure 1.2 Schematic drawings to demonstrate the relationship between the water/cement ratio and porosity	4
Figure 1.3 The concept of corresponding mixes	6
Figure 1.4 Relation between flow table spread and water content of concrete with and without superplasticizer	10
Figure 1.5 Effect of superplasticizer on cement A: Cement + water + superplasticizer B: Cement + water	11
Figure 1.6 Chemical types of superplasticizers.....	13
Figure 1.7 Schematic representation of a lignosulfonate polyelectrolyte microgel unit.....	14
Figure 1.8 Synthesis of SNF from naphthalene	15
Figure 1.9 Synthesis of SMF from melamine	16
Figure 1.10 Chemical structure of polycarboxylate admixture	17
Figure 1.11 Flocculation of cement particles.....	18
Figure 1.12 Schematic representation of slump test.....	22
Figure 2.1 Schematic representation of zeta potential	29
Figure 2.2 Schematic representation of flexural strength measurement test	32
Figure 2.3 Schematic representation of compressive strength test.....	34
Figure 2.4 The chemical structure of SSAMA	35
Figure 2.5 The synthesis of PEG grafted SSAMA.....	36
Figure 2.6 Schematic representation of the mixture of Li ⁺ salts and SSAMA	37
Figure 3.1 FTIR spectrum of SSAMA.....	39

Figure 3.2 FTIR spectrum of A31	39
Figure 3.3 The comparison of FTIR spectra of SSAMA and A31	40
Figure 3.4 FTIR spectrum of B82	41
Figure 3.5 ¹ H NMR spectrum of SSAMA copolymer	42
Figure 3.6 ¹³ C NMR spectrum of SSAMA copolymer	43
Figure 3.7 ¹ H NMR spectrum of A33	44
Figure 3.8 ¹³ C NMR spectrum of A33	44
Figure 3.9 ¹ H NMR spectrum of B55	45
Figure 3.10 ¹³ C NMR spectrum of B55	46
Figure 3.11 The plot of η_{sp}/C vs. C for SSAMA	47
Figure 3.12 The plot of η_{sp}/C vs. C for A32 and A41	48
Figure 3.13 The plot of η_{sp}/C vs. C for B64 and B82	49
Figure 3.14 Effects of superplasticizers on the zeta potential of cement particle surface (X: LiCl, Y: Li ₂ CO ₃ , Z: Li ₂ SO ₄)	50
Figure 3.15 Steric and electrostatic stabilization mechanisms of colloidal dispersions	51
Figure 3.16 Relative slump of PEG2000 grafted SSAMA	53
Figure 3.17 Relative slump of PEG1100 grafted SSAMA	54
Figure 3.18 The relative slump of SSAMA containing various Li salts with different compositions (X= LiCl: SSAMA, Y= Li ₂ CO ₃ : SSAMA, Z= Li ₂ SO ₄ : SSAMA)	55
Figure 3.19 The effects of ion strength on paste fluidity	56
Figure A. 1 FTIR spectrum of A32	68
Figure A. 2 FTIR spectrum of A33	69
Figure A. 3 FTIR spectrum of A41	70
Figure A. 4 FTIR spectrum of B82	71

LIST OF ABBREVIATIONS

ASTM: American Society for Testing and Materials
DVLO: Derjaguin, Verwey, Landau, Overbeek
DMF: Dimethyl formamide
DSC: Differential Scanning Calorimeter
EN: English Standards
FTIR: Fourier Transform Infrared
HSMF: Highly Sulphonated Melamine Formaldehyde
MSA: Methane sulfonic acid
NMR: Nuclear Magnetic Resonance
PC: Polycarboxylate
PEG: Polyethylene glycol
SMF: Sulfonated Melamine Formaldehyde
SNF: Sulfonated Naphthalene Formaldehyde
SP: Superplasticizer
SPF: Sulphonated Phenol Formaldehyde
SSAMA: Poly (4-styrenesulfonic acid-co-maleic acid) sodium salt
TS: Turkish Standards
WRA: Water Reducing Admixtures

CHAPTER 1

INTRODUCTION

1.1. Concrete

Concrete, made from cement, aggregates, chemical admixtures and water, (Figure 1.1) comprises in quantity the largest of all man-made materials. The active constituent of concrete is cement paste and the performance of concrete is largely determined by the cement paste. Admixtures in concrete confer some beneficial effects such as acceleration, retardation, air entrainment, water reduction, plasticity, etc., and they are related to the cement-admixture interaction. Mineral admixtures such as blast furnace slag, fly ash, silica fume, and others, also improve the quality of concrete.

The performance of concrete depends on the quality of the ingredients, their proportions, placement, and exposure conditions. For example, the quality of the raw materials used for the manufacture of clinker, the calcining conditions, the fineness and particle size of the cement, the relative proportions of the phases, and the amount of the mixing water, influence the physicochemical behavior of the hardened cement paste. In the fabrication of concrete, amount and the type of cement, fine and coarse aggregate, water, temperature of mixing, admixture, and the environment to which it is exposed will determine its physical, chemical, and durability behavior. Various analytical techniques are applied to study the effect of these parameters and

for quality control purposes. The development of standards and specifications are, in many instances, directly the result of the work involving the use of analytical techniques [1].

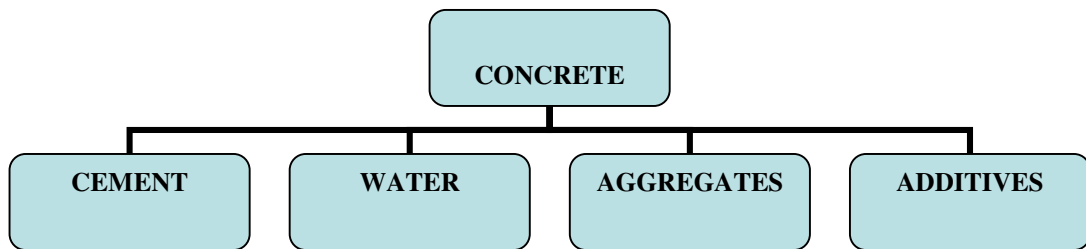


Figure 1.1 The composition of concrete

1.1.1. Cement

Cement, as it is commonly known, is a mixture of compounds made by burning limestone and clay together at very high temperatures ranging from 1400 to 1600 °C [2]. Portland cement is the most common type of cement in general usage. According to ASTM C-150, portland cement is a hydraulic cement produced by pulverizing clinker consisting essentially of hydraulic calcium silicates, usually containing one or more types of calcium sulfate, as an interground addition [1].

Portland cements are multi-component, multi-phasic inorganic materials, comprising major components (Table 1.1) namely tricalcium silicate ($3\text{CaO}\cdot\text{SiO}_2$), dicalcium silicate ($2\text{CaO}\cdot\text{SiO}_2$), tricalcium aluminate ($3\text{CaO}\cdot\text{Al}_2\text{O}_3$), and a ferrite phase of average composition $4\text{CaO}\cdot\text{Al}_2\text{O}_3\cdot\text{Fe}_2\text{O}_3$

which are abbreviated to C_3S , C_2S , C_3A , C_4AF and minor phases (CaO , $CaSO_4 \cdot xH_2O$, Na_2SO_4 , K_2SO_4 , etc.); blended cements include additional components such as supplementary materials (slag, fly ash, silica fume) and fillers (limestone, rock flour, etc.) [1-4].

Table 1.1 Composition of Portland cement with chemical composition and weight percentages

Cement Compound	Weight Percentage	Chemical Formula
Tricalcium silicate	50 %	Ca_3SiO_5 or $3CaO \cdot SiO_2$
Dicalcium silicate	25 %	Ca_2SiO_4 or $2CaO \cdot SiO_2$
Tricalcium aluminate	10 %	$Ca_3Al_2O_6$ or $3CaO \cdot Al_2O_3$
Tetracalcium aluminoferrite	10 %	$Ca_4Al_2Fe_2O_{10}$ or $4CaO \cdot Al_2O_3 \cdot Fe_2O_3$
Gypsum	5 %	$CaSO_4 \cdot 2H_2O$

1.1.2. Water

Water is the key ingredient which, when mixed with cement forms a paste that binds the aggregate together. The water causes the hardening of concrete through a process called hydration. The water needs to be pure in order to prevent side reactions from occurring which may weaken the concrete or otherwise interfere with the hydration process. As reported in many articles [5-6] the role of water is important because the water to cement ratio (w/c) is the most critical factor in the production of "perfect" concrete. Too much water reduces concrete strength, while too little will make the concrete unworkable (Fig 1.2.). Concrete needs to be workable so that it may be consolidated and shaped into different forms (i.e.. walls, domes, etc.). Because concrete must be both strong and workable, a careful balance of the cement to water ratio is required when making concrete [2].

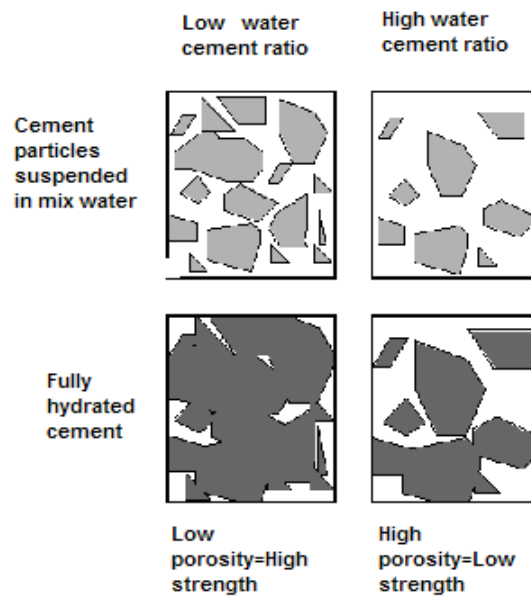


Figure 1.2 Schematic drawings to demonstrate the relationship between the water/cement ratio and porosity

1.1.3. Aggregates

Aggregates are defined as “gravel, sand, slag, crushed rock or similar inert materials” [1]. Fine and coarse aggregates such as river sands and gravels, crushed sands and stones, silica sands, and artificial lightweight aggregates recommended for ordinary cement mortar and concrete are used for latex modified mortar and concrete [7]. The weights of aggregates according to their usages are classified in Table 1.2.

Table 1.2 Classes of Aggregates

Class	Examples of aggregates used	Uses
Ultra-lightweight	vermiculite ceramic spheres perlite	lightweight concrete which can be sawed or nailed, also for its insulating properties
Lightweight	expanded clay shale or slate crushed brick	used primarily for making lightweight concrete for structures, also used for its insulating properties.
Normal weight	crushed limestone sand river gravel crushed recycled concrete	used for normal concrete projects
Heavyweight	steel or iron shot steel or iron pellets	used for making high density concrete for shielding against nuclear radiation

1.1.4. Additives

The water-reducing admixtures are the group of products which possess, as their primary function the ability to produce concrete of a given workability, measured by slump or compacting factor, at a lower water-cement ratio than that of a control concrete containing no admixture.

The earliest known published reference to the use of small amounts of organic materials to increase the fluidity of cement containing compositions, was made in 1932 where polymerized naphthalene formaldehyde sulfonate salts were claimed as useful in this role. This was followed during the mid 1930s to early 1940s by numerous disclosures regarding the use of lignosulfonates and improved compositions.

The normal water-reducing admixtures allow a reduction in the water/cement ratio at a given workability without significantly affecting the setting characteristics of the concrete. Fig. 1.3 summarizes this effect where workability and strength of concrete are discussed on its 28th day.

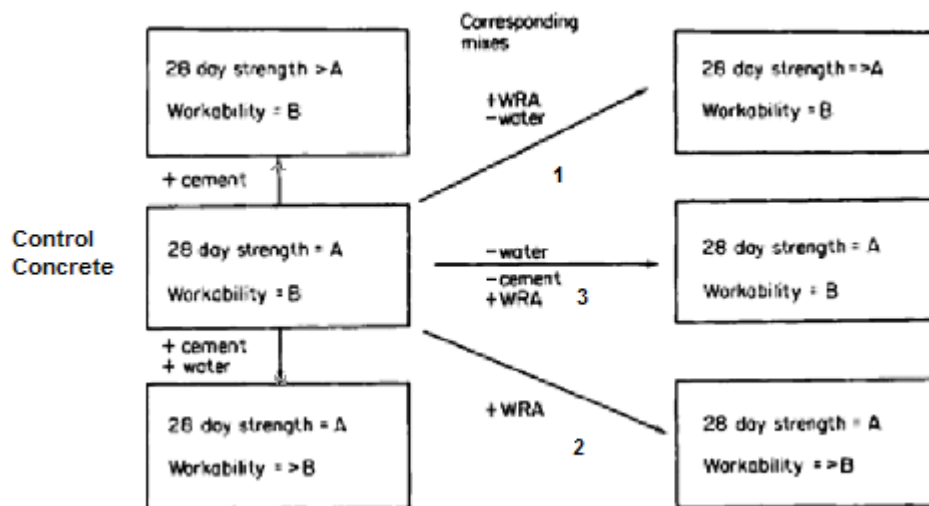


Figure 1.3 The concept of corresponding mixes

In practice, this effect can be utilized in three ways:

1. By the addition of the admixture with a reduction in the water/cement ratio, a concrete having the same workability as the control concrete can be obtained, with unconfined compressive strengths at all ages which exceed those of the control.
2. If the admixture is added directly to a concrete as part of the gauging water with no other changes to the mix proportions, a concrete possessing similar strength development characteristics is obtained, yet having a greater workability than the control concrete.

3. A concrete with similar workability and strength development characteristics can be obtained at lower cement contents than a control concrete without adversely affecting the durability or engineering properties of the concrete.

In all three ways of use, this type of admixture can be regarded as a cement saver. Corresponding mixes are, therefore, concrete mixes having the same workability and 28-day strength characteristics, but the mix containing the water-reducing admixture will have a lower cement content than the other mix.

A list of some admixtures and their functions is given below and summarized in Table 1.3.

The **accelerating** water-reducing admixtures, whilst possessing the water-reducing capability of the 'normal' category, give higher strengths during the earlier hydration period and faster setting times which allow finishing operations to be carried out in a timely manner, particularly at lower temperatures.

The **retarding** water-reducing admixtures again behave in a similar manner to the 'normal' materials and are often of similar chemical composition used at a higher dosage level, but extend the period of time when the concrete is in the plastic state. This means that the time available for transport, handling, placing and finishing is lengthened.

The **air-entraining** water-reducing agents possess the ability to entrain microscopic air bubbles into the cement paste whilst allowing a reduction in the water–cement ratio greater than that which would be obtained by the air entrainment itself [8].

Table 1.3 A table of admixtures and their functions

TYPE	FUNCTION
AIR ENTRAINING	improves durability, workability, reduces bleeding, reduces freezing/thawing problems (e.g. special detergents)
SUPERPLASTICIZERS	increase strength by decreasing water needed for workable concrete (e.g. special polymers)
RETARDING	delays setting time, more long term strength, offsets adverse high temp. weather (e.g. sugar)
ACCELERATING	speeds setting time, more early strength, offsets adverse low temp. weather (e.g. calcium chloride)
MINERAL ADMIXTURES	improves workability, plasticity, strength (e.g. fly ash)
PIGMENT	adds color (e.g. metal oxides)

1.2. Superplasticizers

As reported in many books [8-10] superplasticizers are a special category of water-reducing agents in that they are formulated from materials that allow much greater water reductions, or alternatively extreme workability of concrete in which they are incorporated. This is achieved without undesirable side effects such as excessive air entrainment or set retardation. The materials originally developed as the basis for superplasticizers in the 1960s were sulfonated naphthalene formaldehyde (SNF) and sulfonated melamine formaldehyde (SMF) in Japan and Germany respectively, which have found increasing application world-wide over the intervening years. In the early 1980s, work began on designing polyacrylate-based polymers for superplasticizer formulations and after some difficulties with severe retardation, and in some cases excessive air entrainment, products began to

appear in the marketplace, initially in Germany, and then in Japan and the United States [8].

Superplasticizers increase the workability of mixture and lower water requirement of concrete, so that they lubricate the concrete for facile pumping at high level positions and lead to a concrete of higher compressive strength and improved durability [11]. For these reasons, superplasticizers are classified separately by ASTM C 494-92 [8].

Superplasticizers are water-soluble organic polymers which have to be synthesized, using a complex polymerization process, to produce long molecules of high molecular mass, and they are therefore relatively expensive. On the other hand, because they are manufactured for a specific purpose, their characteristics can be optimized in terms of length of molecules with minimum cross-linking. They also have a low content of impurities so that, even at high dosages, they do not exhibit unduly harmful side effects.

The majority of superplasticizers are in the form of sodium salts but calcium salts are also produced; the latter, however have a low solubility. A consequence of the use of sodium salts is the introduction of additional alkalis into the concrete which may be relevant to the reactions of hydration of the cement and to a potential alkali-silica reaction [9].

1.2.1. Effects of Superplasticizers

The main action of the long molecules is to wrap themselves around the cement particles and give them a highly negative charge so that they repel each other. This results in deflocculation and dispersion of cement particles. The resulting improvement in workability can be exploited in two ways: by

producing concrete with a very high workability or concrete with very high strength. (Fig. 1.4.)

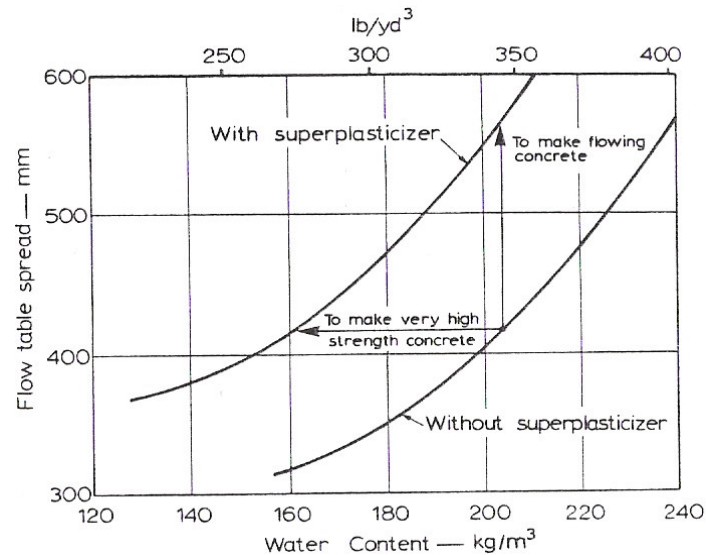


Figure 1.4 Relation between flow table spread and water content of concrete with and without superplasticizer

At a given water/cement ratio and water content in the mix, the dispersing action of superplasticizers increases the workability of concrete, typically by raising the slump from 75 mm (3 in.) to 200 mm (8 in.), the mix remaining cohesive. The resulting concrete can be placed with little or no compaction and is not subject to excessive bleeding and segregation. Such concrete is termed flowing concrete and is useful for placing in very heavily reinforced sections, in inaccessible areas, in floor or road slabs, and also where very rapid placing is desired.

The second use of superplasticizers is in the production of concrete of normal workability but with an extremely high strength owing to a very substantial reduction in the water/cement ratio [9].

The fluidifying effect of the superplasticizer may be envisaged as follows: Portland cement in contact with water has a tendency to flocculate due to Van der Waals' forces, electrostatic interactions between the opposite charges and surface chemical interactions between the hydrating particles. This will result in the formation of agglomeration of particles with open structure with spaces that entrain water molecules. These water molecules are not immediately available for hydration and do not have a lubricating effect. In the presence of a superplasticizer, deflocculation or dispersion of cement particles occurs due to adsorption and electrostatic repulsion. This process does not allow the formation of entrapped water and discourages surface interaction of the particles. Some steric hindrance is possible especially when high molecular weight superplasticizers are used. Such a phenomenon would also prevent particle-particle interactions.

The fluidizing effect of 0.3% SMF on cement is illustrated in Fig. 1.5. While the cement without this admixture appears wet, the paste containing the superplasticizer flows like a liquid [10].

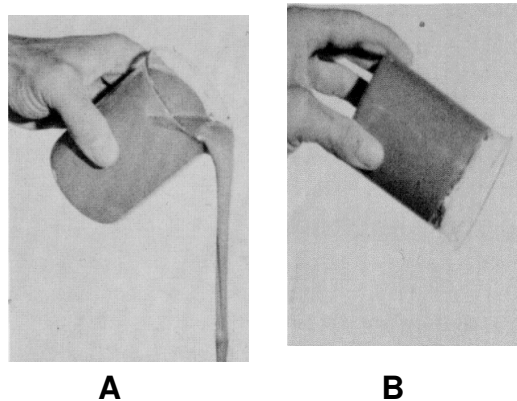


Figure 1.5 Effect of superplasticizer on cement A: Cement + water + superplasticizer B: Cement + water

Using a superplasticizer affects dispersion, adsorption, morphology and rheological properties of the cement. Advantages of introducing superplasticizer in cement would be as follows:

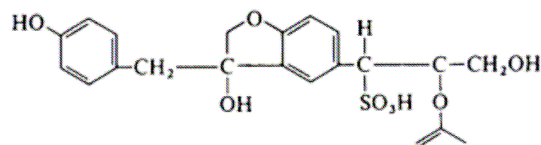
- A rheological property such as viscosity of the concrete is reduced.
- The agglomerates of cement are dispersed into small particles, so the particles become more uniformly dispersed.
- The interaction of chemical additives with cement pastes decreases the concrete porosity and modifies its morphology.
- The compressive strength of concrete is increased.
- The shrinkage of concrete is decreased [11].

1.2.2. Types of Superplasticizers

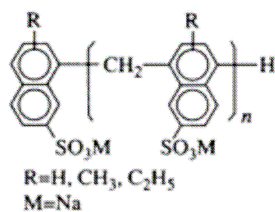
The suitable superplasticizers are divided into six categories:

1. Sodium or calcium lignosulphonate salts.
2. Sulphonated and highly sulphonated melamine formaldehyde condensate products (SMF and HSMF).
3. Sulphonated naphthalene formaldehyde condensate products (SNF).
4. Sulphonated phenol formaldehyde condensate products (SPF).
5. Polyacrylates
6. Carboxylic acid salts.

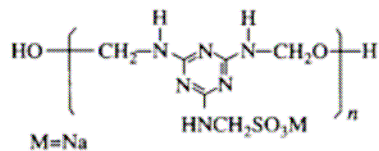
Their structures are shown in Figure 1.6.



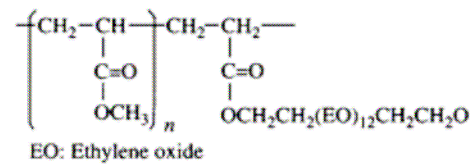
(Repeating unit of a lignosulfonate molecule)



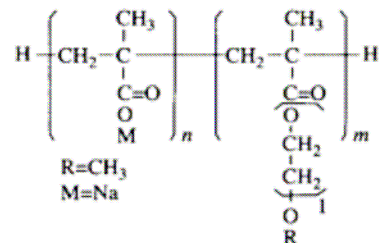
SNF
(Sulfonated naphthalene formaldehyde)



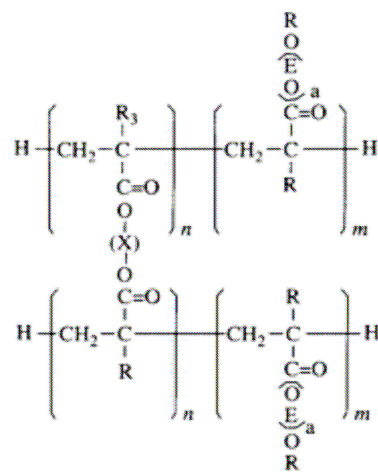
SMF
(Sulfonated melamine formaldehyde)



(Polycarboxylate ester)



(Copolymer of carboxylic acrylic acid with acrylic ester)



(Cross-linked acrylic polymer)

Figure 1.6 Chemical types of superplasticizers

1.2.2.1. Lignosulphonates

Lignin is a complex material which makes up approximately 20% of the composition of wood. During the process for the production of paper-making pulp from wood, a waste liquor is formed as a by-product containing a complex mixture of substances, including decomposition products of lignin and cellulose, sulfonation products of lignin, various carbohydrates (sugars) and free sulfurous acid or sulfates. Subsequent

neutralization, precipitation and fermentation processes produce a range of lignosulfonates of varying purity and composition depending on a number of factors,

such as the neutralizing alkali, the pulping process used, the degree of fermentation and even the type and age of the wood used as pulp feedstock.

It has been found that the lignosulfonate polymer is not a simple linear flexible coiled 'thread', as found in many high molecular weight materials, but forms spherical microgels of the type shown in Fig. 1.7. Thus the charges are predominately on the outside of the spheroid with the internal carboxyl groups and sulfonate group being non-ionized. Conductivity studies have confirmed that lignosulfonates are only 20–30% ionized [8].

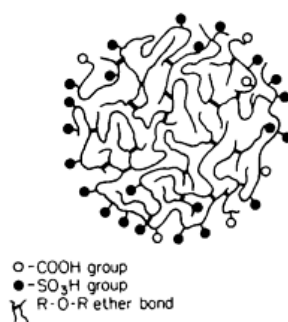


Figure 1.7 Schematic representation of a lignosulfonate polyelectrolyte microgel unit

1.2.2.2. Sulphonated Naphthalene Formaldehyde

This raw material was one of the first materials referred to in the literature as a water-reducing agent yet only since 1970 has it found extensive application in admixture formulations. The material is produced from naphthalene by oleum or sulfur trioxide sulfonation under conditions conducive to the formation of the β sulfonate. Subsequent reaction with formaldehyde leads to polymerization and the sulfonic acid is neutralized with sodium hydroxide or lime. The process is illustrated in Fig. 1.8 [8].

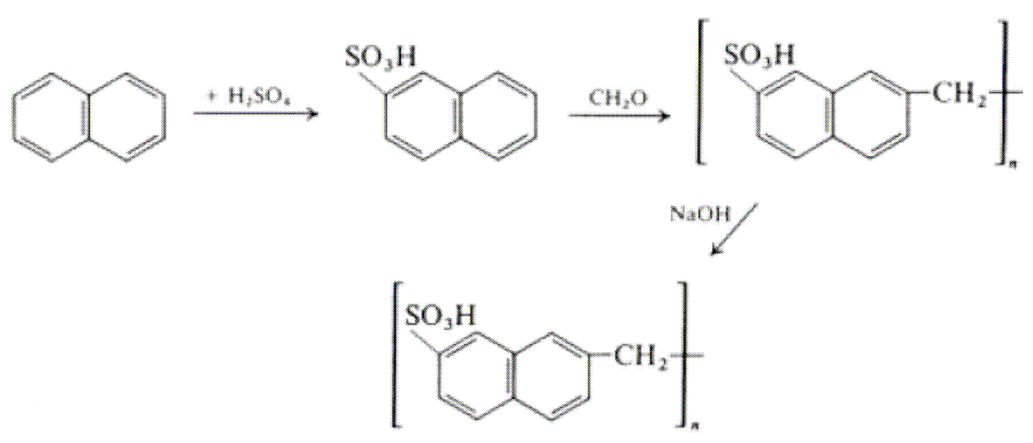


Figure 1.8 Synthesis of SNF from naphthalene

1.2.2.3. Sulphonated Melamine Formaldehyde

This type of chemical product was originally developed in the 1950s as a dispersant for a wide variety of industries, but it was not until some 10 years later that the possibilities for its use in concrete were recognized. It is manufactured by normal resinification techniques according to the process shown in Fig. 1.9 [8].

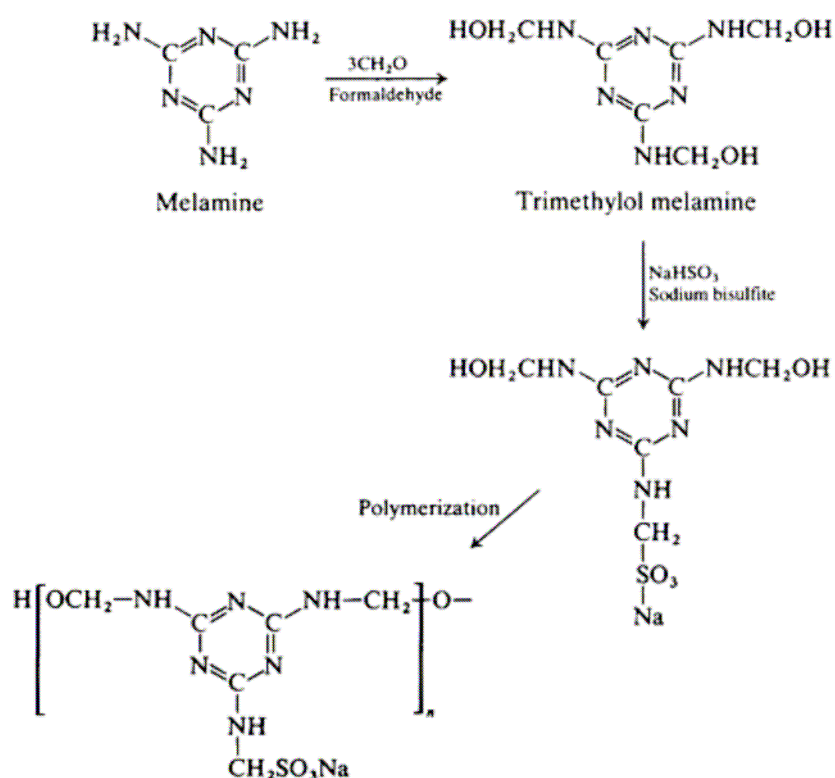


Figure 1.9 Synthesis of SMF from melamine

1.2.2.4. Polycarboxylates

In the late twentieth century new admixtures based on polycarboxylate ethers were developed, with structural characteristics that provided for more fluid concrete, which was more resistant to segregation and exudation than any prepared with the superplasticisers known previously. For these reasons nowadays polycarboxylate admixtures have been introduced into the cement systems replacing admixtures based on melamine and naphthalene. The molecular structure of polycarboxylate (PC) superplasticiser admixtures is shown in Fig. 1.10.

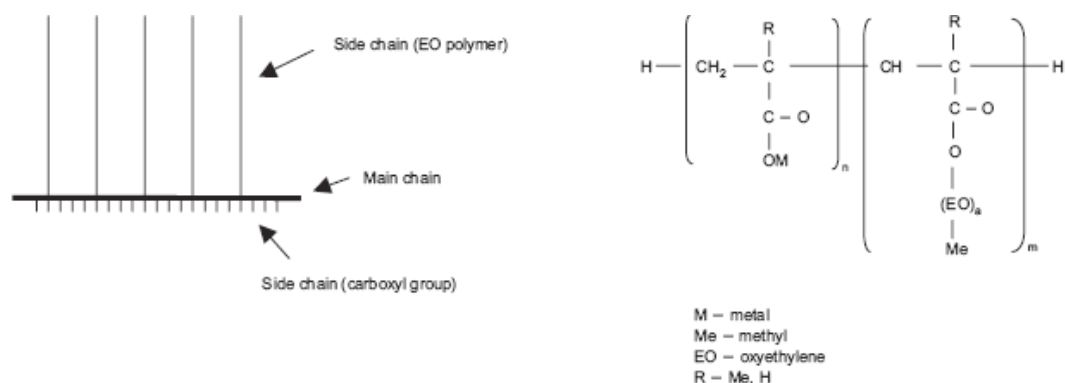


Figure 1.10 Chemical structure of polycarboxylate admixture

Their 'comb-type' molecule consists of one main linear chain with lateral carboxylate and ether groups. According to literature the carboxylate groups are instrumental in the adsorption of these admixtures to cement particles. Dispersion is due to electrostatic repulsion (as in melamine and naphthalene admixtures) owing to the carboxylate groups, but primarily to the steric repulsion associated with the long lateral ether chains. The high degree and duration of the fluidity that this admixture affords concrete are related to structural factors; hence, the shorter the main chain and the longer and more numerous the lateral chains, the greater and more longlasting is the fluidity induced [12]. Yamada et. al., investigated that a higher sulfonic group content in PC type superplasticizers containing sulfonic and carboxylic groups gave higher fluidity at the same dosage [13].

Björnström et. al.; discussed the model for the adsorption of superplasticizer on a cement particle. Superplasticizers are surface active agents. These modify the surface charges on the cement particles and thus make them disperse. Superplasticizers are adsorbed on the hydrating cement particles. This could decrease flocculation in at least three ways:

1. Increase in zeta potential; if all the particles carry a surface charge of the same sign and magnitude, they will repel each other, and will thereby disperse.
2. Increase in solid liquid affinity; if the particles are more strongly attracted to the liquid than to each other; they will tend to disperse.
3. Steric hindrance; the oriented adsorption of a non-ionic polymer can weaken the attraction between solid particles. The hydration process leads to the formation of open network voids Fig. 1.11. These particles are deflocculated by the addition of superplasticizers [14].

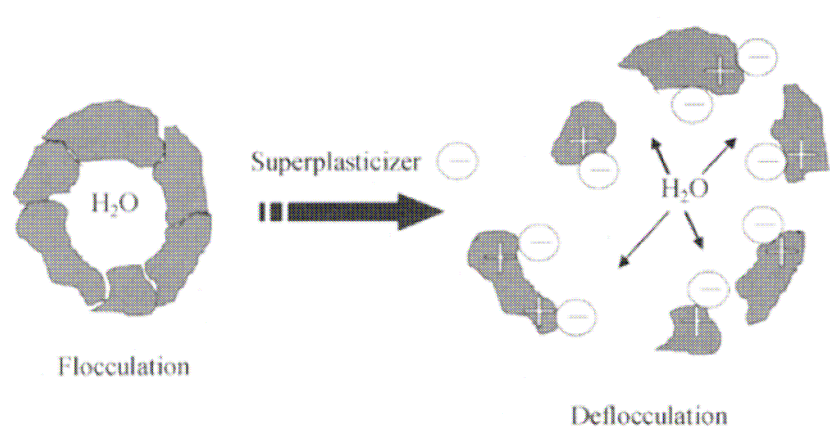


Figure 1.11 Flocculation of cement particles

The dispersion mechanism is dependent upon the type of superplasticizer adsorbed on the surface. Basically, there are two types of dispersion mechanisms: electrostatic repulsion and steric hindrance. Sulfonated superplasticizers induced a negative charge on cement particles dispersing them by electrostatic repulsion, whereas with the polycarboxylate based polymer the dispersion mechanism is mainly controlled by steric hindrance. It

was understood from the zeta potentials for the slurries containing sulfonated superplasticizers are very negative.

Uchikawa et al. [15] and Yoshioka [16] reported that sulfonated superplasticizers give rise to a higher negative zeta potential than polycarboxylate acid-based superplasticizers. The polycarboxylate copolymer is made up of a backbone, with carboxylic groups, and polyoxyethylene side chains. These long side chains contribute to the role of steric hindrance in the case when polycarboxylate superplasticizer is used. It is believed that the adsorption of this kind of copolymer on cement particles occurs via carboxylic acid groups. The lignosulfonate, sulfonated melamine and sulfonated naphthalene-type superplasticizers have a lower molecular mass than the polycarboxylate type and have no long side chains [14]. However Ohta et al. pointed out that the cement-dispersing effect could not be explained simply by changes in steric repulsion due to the graft chain length, but that it strongly depends on chemical structure such as geometrical balance between the main chain and graft chains. However the effect of chemical structure on the dispersing effect of graft copolymers has not yet been understood quantitatively [17].

Andersen and Roy [18] have reported that sulfonated polymers of naphthalene, melamine and polystyrene with largest molecular weight gives the largest negative zeta potential, and is therefore concluded to have higher dispersing capability. The absence of long side chains provide the smaller sulfonated polymers with a higher charge density than the heavier polycarboxylate type polymer, therefore the electrostatic repulsion is more pronounced.

Superplasticizers have varied reactivity, depending upon their chemical configuration and molecular weight. Their reactivity or ability to disperse cement particles also depends upon the type of cement used. Björnstrom et

al. investigated that one type of cement does not behave in the same way with different superplasticizer and one superplasticizer does not behave in the same way with different cements. It is a dilemma and headache for the superplasticizer producers [14].

1.2.3. Applications of Superplasticizers

Superplasticizers are not only of interest in the concrete industry. They have a much larger scale of application, particularly in ceramic processing. Traditional ceramics (whitewear, sanitary appliances, insulators, etc.), refractories (crucibles, engine components, supports for catalysts, etc.), bioceramics, biocements, watchmaking (watch bodies) are some of the examples of products which include the use of superplasticizers in their production scheme [19].

1.3. Concrete Properties

1.3.1. Workability

The quality of fresh concrete is determined by the ease and homogeneity with which it can be mixed, transported, compacted and finished. It has also been defined as the amount of internal work necessary to produce full compaction. A good workable concrete should not exhibit excessive bleeding and segregation. Thus workability includes properties such as flowability, moldability, cohesiveness and compactibility. One of the main factors

affecting workability is the water content in the concrete mix. A harsh concrete becomes workable by the addition of water. Workability may also be improved by the addition of plasticizers and air-entraining agents. The factors that affect workability include quantities of paste and aggregates, plasticity of the cement paste, maximum size and grading of the aggregates, and shape and surface characteristics of the aggregate.

Another term that has been used to describe the state of fresh concrete is consistency of fluidity. It describes the ease with which a substance flows. The term consistency is sometimes used to describe the degree of wetness of concrete. Wet concrete is more workable than the dry concrete. A concrete having the same consistency may, however have different workability characteristics.

Although several methods have been suggested to determine workability, none is capable of measuring this property directly. It is therefore usual to measure some type of consistency as an index of workability. The most extensively used test is the slump test. This method is described by the ASTM C143. The slump test uses a frustum of cone 300 mm (12 in.) high. (Fig. 1.12) Concrete is filled in this cone and the cone is lifted slowly and the decrease in the height of the center of the slumped concrete is measured. For structural concrete, a slump of 75-100 mm (3-4 inches) is sufficient for placement in forms [10].

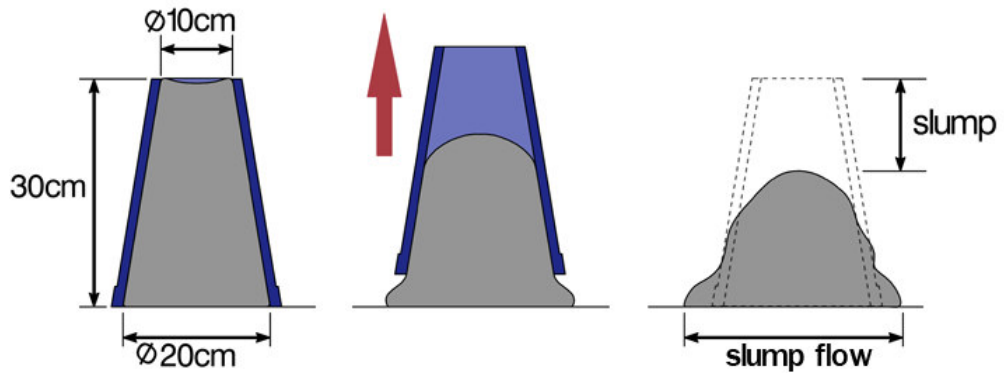


Figure 1.12 Schematic representation of slump test

1.3.2. Setting

The setting of concrete is determined by using the mortar contained in it. A penetrometer is used for determining the initial and final setting times of mortar. A needle of appropriate size has to be used. The force required to penetrate 1 inch in depth is noted. The force divided by the area of the bearing surface of the needle yields the penetration resistance. The initial setting time is the elapsed time, after the initial contact of cement and water, required for the mortar sieved from the concrete to reach a penetration resistance of 500 lbs/sq.in. (3.5 MPa). The corresponding resistance for the final setting time is 4000 lbs/sq.in. (27.6 MPa) [10].

1.3.3. Bleeding and Segregation

In a freshly placed concrete which is still plastic, settlement of solids is followed by the formation of a layer of water on the surface. This is known as bleeding or water gain. Bleeding is not necessarily harmful. If undisturbed, the water evaporates so that the effective water/cement ratio is lowered with

a resultant increase in strength. Bleeding characteristics are measured by bleeding rate or bleeding capacity, applying the ASTM C232 standard. In this method, the relative amount of mix water that appears on the surface of concrete placed in a cylindrical container is measured. At specified intervals, the water accumulating on the surface is determined until bleeding ceases. The top surface of concrete subsides during bleeding causing what is known as plastic shrinkage.

During the handling of a concrete mixture, there may be some separation of coarse aggregates from the mixture, resulting in a nonuniform concrete mass. This is known as segregation. The primary cause of segregation is the differences in the size of the particles and specific gravity of the mix. The tendency to segregate increases with slump, reduction in cement content, or increase in the maximum size and amount of aggregate. By proper grading of the constituents and handling, this problem can be controlled [10].

1.3.4. Mechanical Properties

The hardened concrete has to conform to certain requirements for mechanical properties. They include compressive strength, splitting tensile strength, flexural strength, static modulus of elasticity, Poisson's ratio, mechanical properties under triaxial loads, creep under compression, abrasion resistance, bond development with steel, penetration resistance, pull out strength, etc.

The mechanical behavior of concrete should be viewed from the point of view of a composite material. A composite material is a three dimensional combination of at least two chemically and mechanically distinct materials with a definite interface separating the components. This multiphase material will have different properties from the original components.

The factors that influence the mechanical behavior of concrete are: shape of particles, size and distribution of particles, concentration, their orientation, topology, composition of the disperse and continuous phases, and that between the pore structure.

The strength of concrete depends on the strength of the paste, coarse aggregate, and the paste-aggregate interface. This interface is the weakest region of concrete and is where the failure occurs before its occurrence on the aggregate or the paste. The weakness of this interface is due to weak bonding and the development of cracks which may develop due to bleeding and segregation and volume changes of the cement paste during setting and hydration [10].

1.4. Aim of the Study

The aim of this research is to synthesize and characterize a novel water-soluble anionic polyelectrolyte that can be used as a superplasticizer in concrete, and to investigate the effects of degree of PEG grafting and the various Li salts of the polycarboxylate copolymer on the fluidity and mechanical properties in concrete. The zeta potential values give an idea about the dispersion mechanism of the cement paste.

CHAPTER 2

EXPERIMENTAL

2.1. Chemicals

Poly (4-styrenesulfonic acid-co-maleic acid) sodium salt 3:1 (styrenesulfonic acid: maleic acid mol ratio) (MW: 20000 g/mol) (Aldrich), polyethylene glycol 2000 monomethyl ether (Fluka), polyethylene glycol 1100 monomethyl ether (Fluka), methane sulfonic acid (MSA) (Merck), distilled water, dimethylformamide (Merck), 1,4-dioxane (Merck), toluene (Merck), lithium sulfate (Aldrich), lithium carbonate (Aldrich), lithium chloride (Sigma-Aldrich), Portland cement (CEM I 42.5R), tap water were used as such.

2.2. Instrumentation

2.2.1. Fourier Transform Infrared Spectroscopy

FTIR spectra of the polymers were recorded on a Nicolet 510 FT-IR spectrophotometer in the wave number range 400-4000 cm^{-1} . The polymer samples were pounded into powder in a mortar, mixed with KBr, and pressed into pellets.

2.2.2. Nuclear Magnetic Resonance (NMR)

Both ^1H and ^{13}C spectra of the polymers were recorded on Bruker-Spectrospin Avance DPX 400 high performance digital FT-NMR spectrometer. D_2O was used as the solvent and tetramethylsilane was used as the internal standard. The ppm scale was used to designate the chemical shifts δ .

2.2.3. Dilute Solution Viscosimetry

Viscosity of a polymer solution depends partly on concentration and size, which itself is related to the molecular weight, (i.e., molecular weight) of the dissolved polymer. By measuring the solution viscosity it is possible to get an idea about molecular weight. For polydisperse linear polymers the viscosity-average molecular weight M_v is given by the Mark Houwink equation.

$$[\eta] = k M_v^a \quad (2.1)$$

Viscosity measurements were performed by Ubbelohde viscometer using distilled water as a solvent in a constant temperature bath of 25°C and the time of flow was measured with a stopwatch.

2.2.4. Zeta Potential

Zeta potential is a physical property which is exhibited by any ionic particle in suspension. It can be used to optimize the formulations of suspensions and

emulsions. Knowledge of the zeta potential can reduce the time needed to produce trial formulations. It is also an aid in predicting long-term stability.

Derjaguin, Verwey, Landau and Overbeek developed a theory (DVLO theory) in the 1940s which deals with the stability of colloidal systems. DVLO theory suggests that the stability of a particle in solution is dependent upon its total potential energy function V_T . This theory recognizes that V_T is the balance of several competing contributions:

$$V_T = V_A + V_R + V_S \quad (2.2)$$

where V_S is the potential energy due to the solvent, V_A and V_R , are the attractive and repulsive contributions due to particle-particle interactions. These contributions potentially are much larger and operate over a much larger distance. The attractive potential is given by;

$$V_A = -A/(12 \pi D^2) \quad (2.3)$$

where A is the Hamaker constant and D is the particle separation. The repulsive potential V_R is a far more complex function.

$$V_R = 2 \pi \epsilon a \xi^2 \exp(-\kappa D) \quad (2.4)$$

where a is the particle radius, π is the solvent permeability, κ is a function of the ionic composition and ξ is the zeta potential.

DVLO theory suggests that the stability of a colloidal system is determined by the sum of these Van der Waals attractive (V_A) and electrical double layer repulsive (V_R) forces that exist between particles as they approach each other due to the Brownian motion they are undergoing. This theory proposes that an energy barrier resulting from the repulsive force prevents two particles approaching one another and adhering together. But if the particles

collide with sufficient energy to overcome that barrier, the attractive force will pull them into contact where they adhere strongly and irreversibly together. Therefore if the particles have a sufficiently high repulsion, the dispersion will resist flocculation and the colloidal system will be stable. However if a repulsion mechanism does not exist then flocculation or coagulation will eventually take place.

The development of a net charge at the particle surface affects the distribution of ions in the surrounding interfacial region, resulting in an increased concentration of counter ions (ions of opposite charge to that of the particle) close to the surface. Thus an electrical double layer exists around each particle. The liquid layer surrounding the particle exists as two parts; an inner region, called the Stern layer, where the ions are strongly bound and an outer, diffuse, region where they are less firmly attached. Within the diffuse layer there is a notional boundary inside which the ions and particles form a stable entity. When a particle moves (e.g. due to gravity), ions within the boundary move with it, but any ions beyond the boundary do not travel with the particle. This boundary is called the surface of hydrodynamic shear or slipping plane. The potential that exists at this boundary is known as the Zeta potential [21]. (Fig. 2.1)

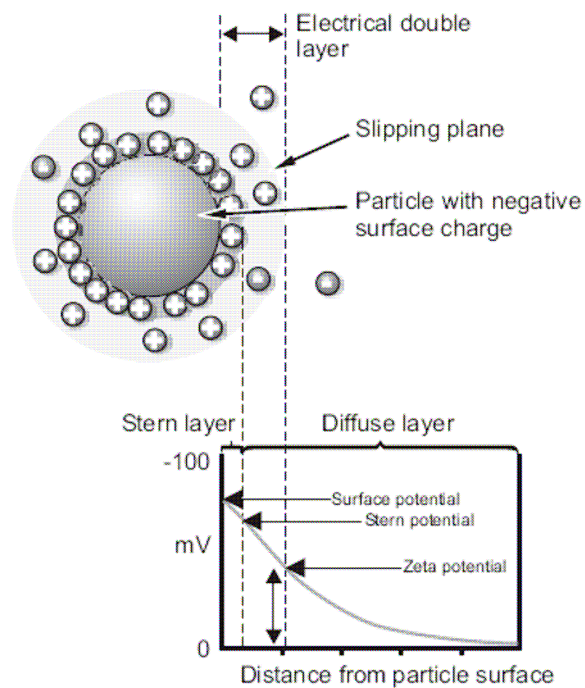


Figure 2.1 Schematic representation of zeta potential

Zeta potentials were measured using the following method: 0.1 g superplasticizer was dissolved in 81.6 g tap water in a beaker. After complete dissolution, 50 g Portland cement was added, mixed and left overnight for the sedimentation of cement particle. The solution above the cement paste was then filtered through Por.4 Gooch crucible. The pH of all slurries was measured and found to be 13.5 in all cases. The slurry was then transferred to the measuring cell and the temperature was set to 25°C. The zeta potential of the samples was measured with a Malvern Nano ZS90 Instrument.

2.2.5. Mini Slump Test

When investigating the effect of a large number of admixtures on the workability of cement, mortar or individual cement mineral phases, it is very quick and economical to use the mini slump method. The difference between the slump test and the mini-slump test is the dimensions of the mold filled up with the cement paste or concrete. In concrete, a conical mold is used with a height of 30 cm, upper diameter of 10 cm and a bottom diameter of 20 cm, however in mini slump test; the mold has a height of 6 cm, upper diameter of 7 cm and a bottom diameter of 10 cm.

Cement pastes were mixed at 25 °C and at w/c of 0.4, using an ELE International Automatic/Manual Mortar Mixer. The cement used in these tests is Portland cement (CEM I 42.5R) as defined by TS EN 197-1. First, SP (1.2 g) and water (244.8 g) were mixed and put into a bowl. Then 600 g cement was added and mixed for 1 min at low speed and a further 3 min at high speed. The cone was filled with the cement paste and the cone was lifted slowly to allow the paste to flow. The maximum diameter of the spread sample and the maximum width perpendicular to that diameter were measured after 30 s in accordance with ASTM C 143. The average of these values was defined as the flow value. Finally the relative slump was calculated by the following formula:

$$\Gamma_m = (d / d_0)^2 - 1 \quad (2.5)$$

where d_0 is the initial diameter of the cone, and d is the final diameter of mortar and Γ_m is the relative flow of the paste [21]. To correlate the results, a blank was prepared from 600 g Portland Cement and 244.8 g water.

2.2.6. Mechanical Measurements of Mortars Prepared with Polymer Samples

2.2.6.1. Flexural Strength Measurements

Solutions used for the mini-slump tests were re-prepared for the flexural strength measurements of the samples, too. 225 grams of these solutions were taken and mixed with 1350 g standard sand mixture and 450 g Portland cement. The mixture is called mortar. The molds with dimensions of 4x4x16 were filled with these mixtures. From the mixture, it is possible to fill three molds. Flexural strength tests were performed with these mortars in accordance with TS EN 196-1.

The instrument used for determining flexural strength was a Losen Hausen Loading Frame. It had a capacity of 1,000 kilogram force (kgf) for flexural strength tests.

After removing the mortar samples from the mold, they were put in the loading frame as shown in Fig. 2.2. The total length of the bar is 16 cm, the length of the support span is 12 cm, the height and the width of the bar is 4 cm.

The length of the bar on which the force was applied is 12 cm. The cross-sectional area of the bar is $4 \times 4 = 16 \text{ cm}^2$.

The flexural strength of a material σ_{flex} is given by:

$$\sigma_{\text{flex}} = \frac{\mu \cdot C}{I} \quad (2.6)$$

Where;

μ = moment due to the applied force

c = the distance from the neutral axis to the bottom fiber for the x-section

I = moment of inertia of a square prism $= \frac{1}{12}bd^3$

b = width of the bar

d = height of the bar

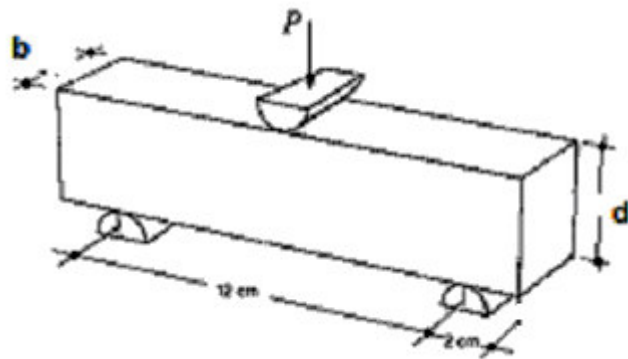


Figure 2.2 Schematic representation of flexural strength measurement test

If $c = d/2$,

$$\sigma_{flex} = \frac{\mu \cdot \frac{d}{2}}{\frac{1}{12} \cdot bd^3} \quad (2.7)$$

Where,

$$\mu = \frac{P \cdot L}{4} \quad (2.8)$$

P = the load (force) at the fracture point (flexural stress)

L = the length of the support span

Then,

$$\sigma_{flex} = \frac{\frac{P \cdot L}{4} \cdot \frac{d}{2}}{\frac{1}{12} \cdot b d^3} \quad (2.9)$$

Since $b=d$;

$$\sigma_{flex} = \frac{\frac{P \cdot L}{4} \cdot \frac{d}{2}}{\frac{1}{12} \cdot d^4} \quad (2.10)$$

When the equation is simplified,

$$\sigma_{flex} = \frac{3}{2} \cdot \frac{P \cdot L}{d^3} \quad (2.11)$$

This equation was used for calculating the flexural strength of the samples [22-23]. The unit of the load applied is kgf, so the unit of the flexural strength will be kgf/cm² and in terms of N/mm².

2.2.6.2. Compressive Strength Measurements

The compressive strength tests were performed on the broken pieces of the mortar samples according to the TS EN 196-1. The machine used for the determination of the compressive strength is ELE universal compressive testing machine with a capacity of 300,000 kgf.

4x4x4 cubic mortar samples, which were the samples from the flexural strength tests, were put in compressive test machine as shown in Fig. 2.3.

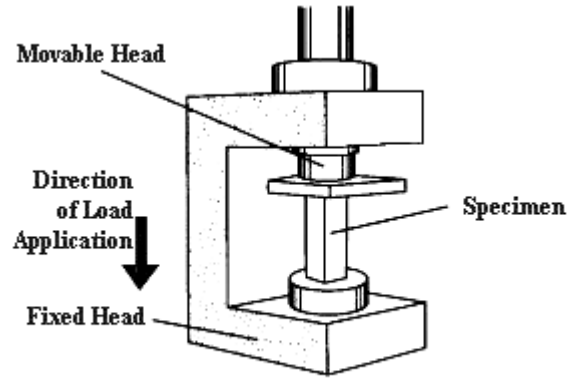


Figure 2.3 Schematic representation of compressive strength test

The compressive strength of the mortar samples was calculated by the equation below:

$$\sigma = \frac{F}{A_0} \quad (2.12)$$

where F is the load, A_0 is the cross-sectional area of the bar. While inserting the data for the calculation of σ and σ_{flex} , TS EN 196-1 standard is also used.

2.3. Synthesis

2.3.1. Synthesis of Poly (ethylene glycol) monomethyl ether-g-poly(4-styrenesulfonic acid-co-maleic acid)sodium salt (SSAMA-g-PEG)

Desired amounts of PEG and SSAMA were dissolved in minimum amount of distilled water (i.e. approximately 15 ml) and diluted with 150 ml of DMF. The solution was refluxed in a round bottom flask with methane sulfonic acid as a catalyst, at 90 °C, for 7 hours, in oil bath. Then the mixture was precipitated in 1,4-dioxane, filtered and dried till constant weight in oven at 50 °C [24].

The grafting reaction was carried out by using two different PEGs with molecular weights 2000 and 1100. The molecular weight of repeating unit of SSAMA was 712.561 g/mol. The grafted copolymers thus synthesized were referred as SSAMA-PEG2000 and SSAMA-PEG1100. Their composition ratios were tabulated in Table 2.1. The chemical structure of SSAMA is illustrated in Fig. 2.4.

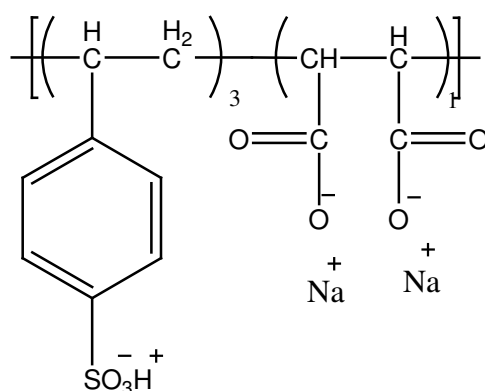


Figure 2.4 The chemical structure of SSAMA

Table 2.1 The composition ratios of monomers used in the preparation of PEG grafted copolymers

Polymer ID	Monomers	Weight ratio (w/w)	Mol ratio (n/n)
A31	SSAMA/PEG2000	3:1	4.21:0.5
A32	SSAMA/PEG2000	3:2	4.21:1.0
A33	SSAMA/PEG2000	3:3	4.21:1.5
A41	SSAMA/PEG2000	4:1	5.61:0.5
B62	SSAMA/PEG1100	6:2	8.42:1.82
B64	SSAMA/PEG1100	6:4	8.42:3.64
B55	SSAMA/PEG1100	5:5	8.42:4.55
B82	SSAMA/PEG1100	8:2	11.23:1.82

The grafting reaction is illustrated in Figure 2.5.

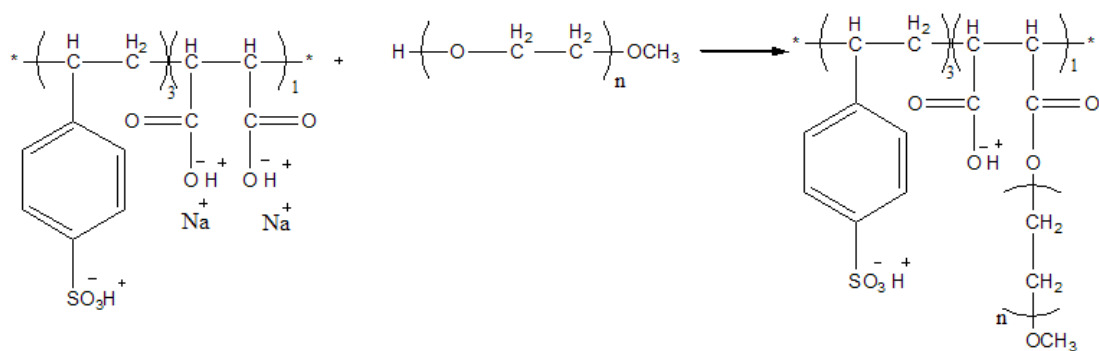


Figure 2.5 The synthesis of PEG grafted SSAMA

2.3.2. Adding Different Li⁺ Salts into the Medium

The calculated moles of SSAMA (1.2 g) was mixed with LiCl, Li₂CO₃ or Li₂SO₄ in the stoichiometry of 2:1 (SSAMA:Li⁺ salt), 1:1 and excess (threefold mol ratio of SSAMA) in a beaker with 244.8 g tap water. (Table 2.2) The solutions were mixed continuously and left overnight. The samples were kept for minislump loss test.

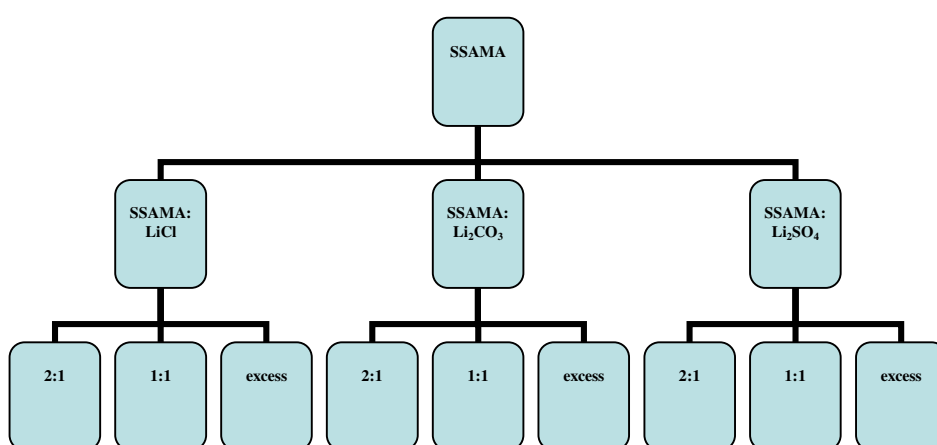


Figure 2.6 Schematic representation of the mixture of Li⁺ salts and SSAMA

CHAPTER 3

RESULTS AND DISCUSSION

3.1. Characterization of the Polymers

3.1.1. FTIR Results

The structures of PEG grafted SSAMA copolymers were confirmed by using FTIR spectroscopy. Figure 3.1 shows that FTIR spectrum of SSAMA. The FTIR spectrum of SSAMA shows the following adsorption bands: 3443.71 cm^{-1} (acid O-H), 2932.25 cm^{-1} (C-H stretching), 1583.05 cm^{-1} (C=O stretching overlapped with C=C aromatic stretching of styrene), 1496.25 cm^{-1} (C-H bending), 1412.22 cm^{-1} (S=O stretching), 1039.42 and 1008.90 cm^{-1} (C-O stretching).

Figure 3.2 shows the FTIR spectrum of A31. The adsorption bands are: 3443.99 cm^{-1} (O-H stretching), 2923.09 cm^{-1} (C-H stretching), 1716.85 cm^{-1} (C=O stretching of ester), 1601.20 cm^{-1} (C=C aromatic stretching), 1496.28 cm^{-1} (C-H bending), 1412.90 cm^{-1} (S=O stretching), 1038.86 and 1009.47 cm^{-1} (C-O stretching). The FTIR spectra of A32, A33 and A41 are given in the Figs A.1, A.2, A.3 in the appendix.

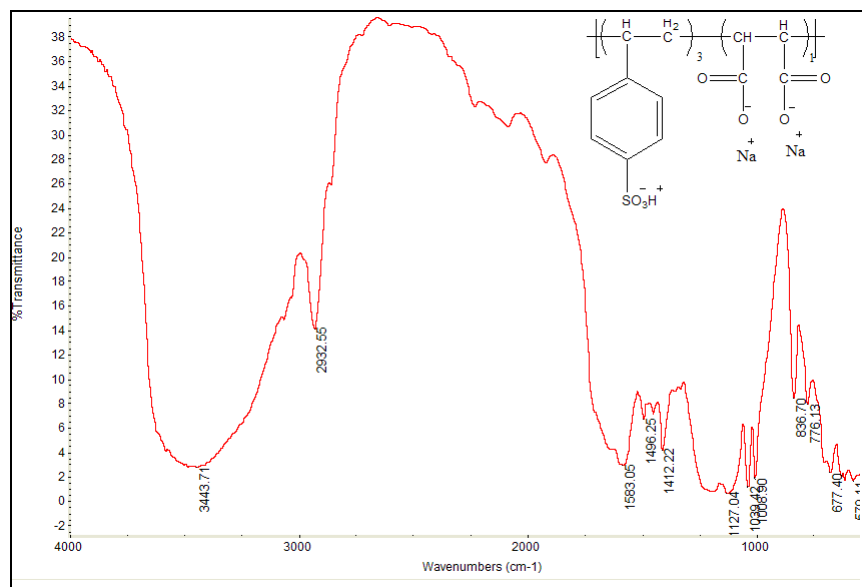


Figure 3.1 FTIR spectrum of SSAMA

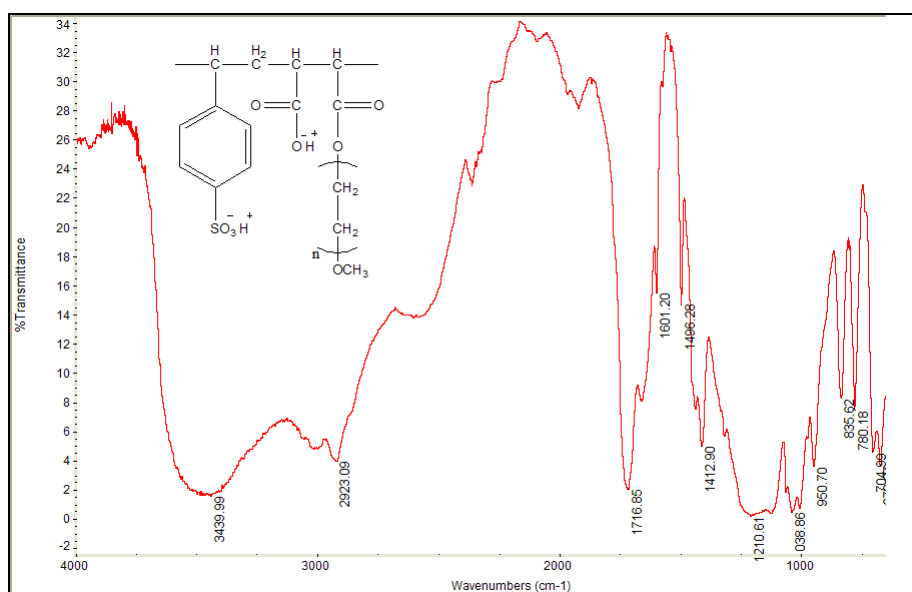


Figure 3.2 FTIR spectrum of A31

The comparison of FTIR spectra of SSAMA and A31 copolymers is illustrated in Fig. 3.3. The sharp peak at 1716.85 cm^{-1} belongs to C=O stretching of ester group proves the successful grafting of PEG to SSAMA. The sharp peak at 1496.28 cm^{-1} is related to C-H bending of CH_2 groups and the peak at 2923.09 cm^{-1} shows C-H stretching of CH_2 groups in the side chain.

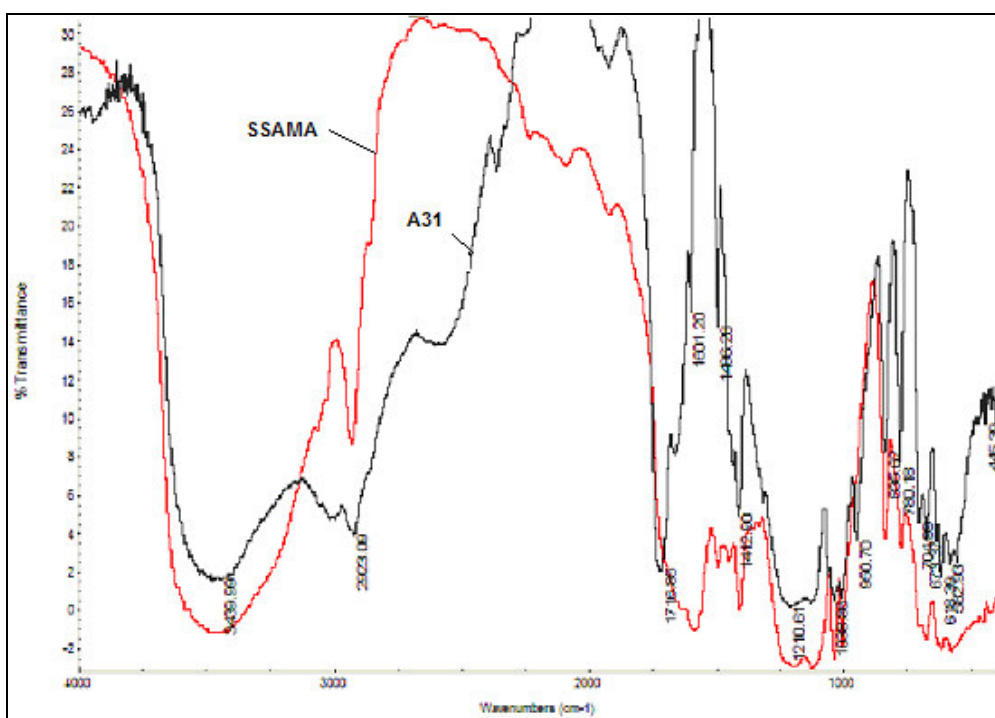


Figure 3.3 The comparison of FTIR spectra of SSAMA and A31

Fig. 3.4 shows the FTIR spectrum of B82. Similar absorption peaks are observed with weaker band at 1496.25 cm^{-1} corresponding to C-H stretching and at 2931.83 cm^{-1} corresponding to C-H bending in PEG which is expected. The intensity of C=O stretching vibration of ester group at 1721

cm^{-1} is not very strong as in the spectra of A31. The FTIR spectrum of B82 is given in the Fig. A.4 in the appendix.

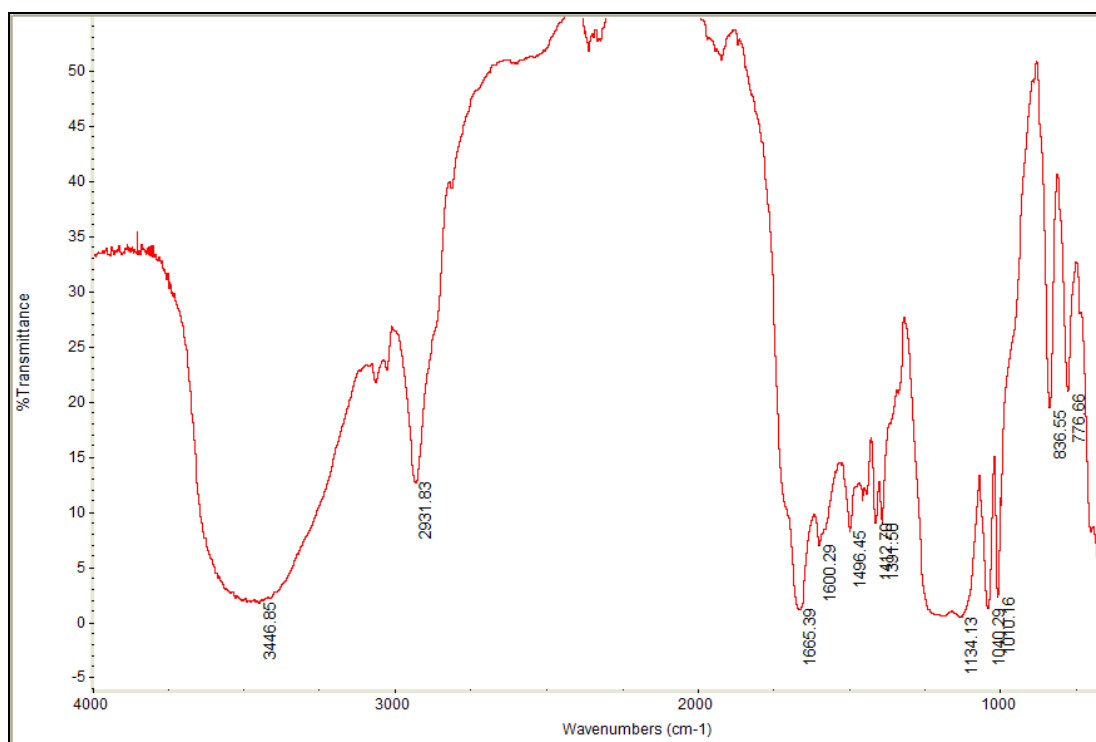


Figure 3.4 FTIR spectrum of B82

3.1.2. NMR Results

3.1.2.1. ^1H NMR and ^{13}C NMR Characterization of SSAMA

Fig. 3.5 shows ^1H NMR spectrum of SSAMA. The chemical shifts of SSAMA are: δ 7.6-6.75 (6H) (5), 2.11 (1H) (4), 1.63 (2H) (3), 4.0 (1H) (2), 3.75 (1H) (1)

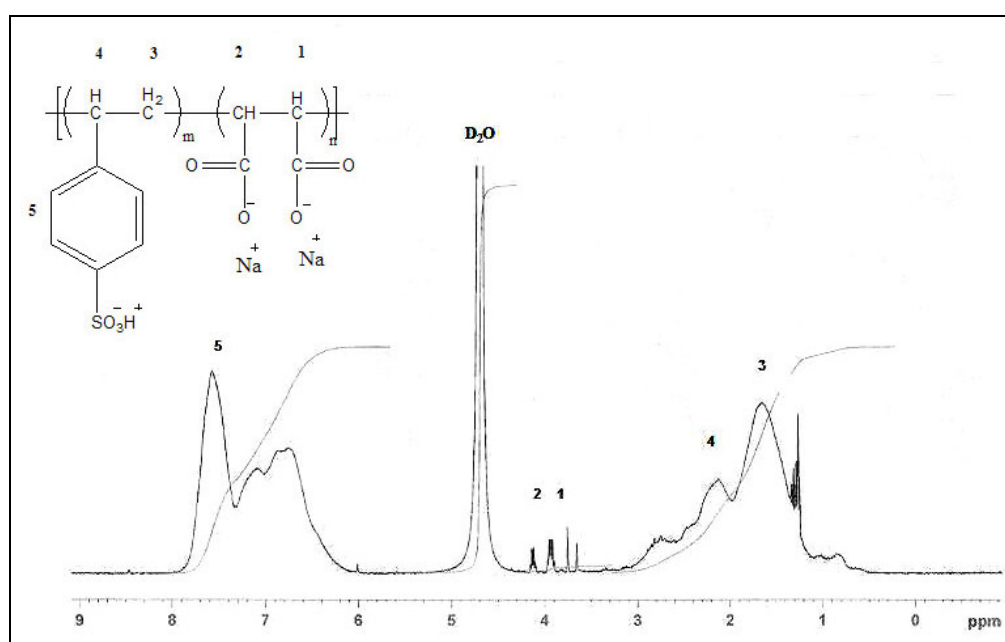


Figure 3.5 ^1H NMR spectrum of SSAMA copolymer

Figure 3.6 shows decoupled ^{13}C NMR spectrum of SSAMA. The chemical shifts are: δ 180 (1C,2C), 147-98 (3Ar), 60-70 (5C, 6C), 44-40 (4C), 15 (5C)

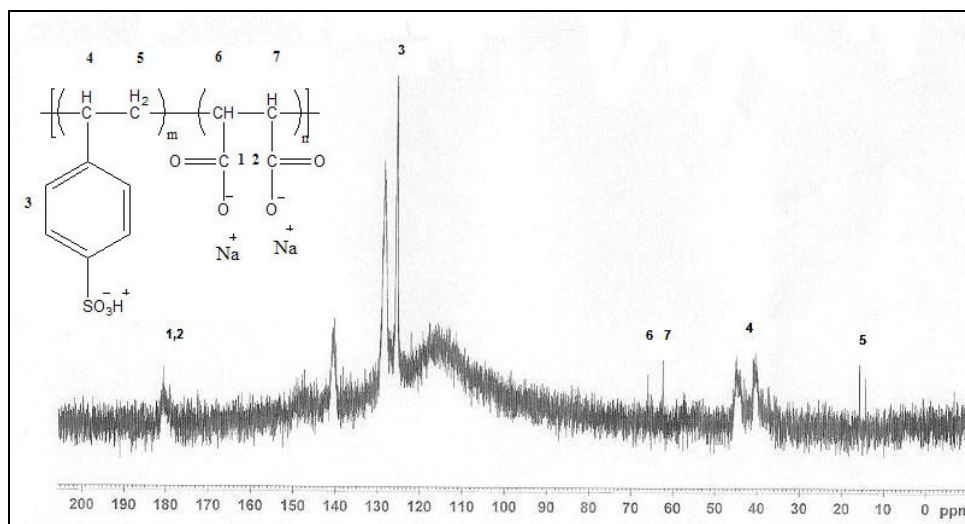


Figure 3.6 ^{13}C NMR spectrum of SSAMA copolymer

3.1.2.2. ^1H and ^{13}C NMR Characterization of A33

Fig. 3.7 and Fig. 3.8 represents ^1H and ^{13}C NMR spectra of A33 respectively. The chemical shifts of A33 are as follows: δ 7.61 (6H) (1), 3.60 (4H) (2), 2.65 (3H) (3) in ^1H NMR spectrum and δ 176 (1C,2C), 147-113 (3Ar), 40 (4C), 39 (5C) 58-60 (6-7-9), 69 (8C) in ^{13}C NMR spectrum.

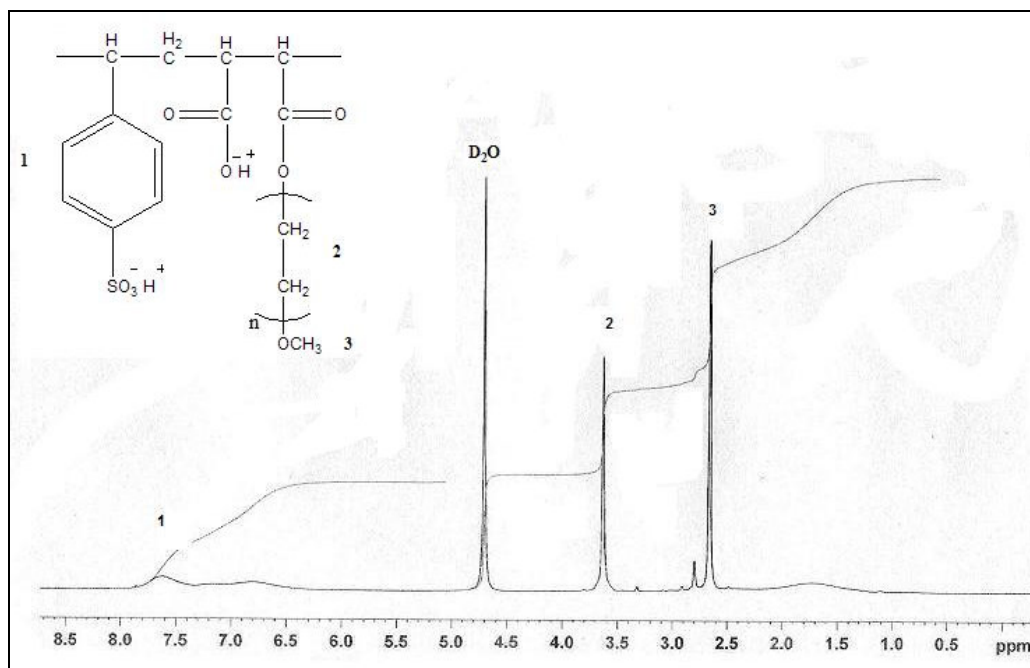


Figure 3.7 ¹H NMR spectrum of A33

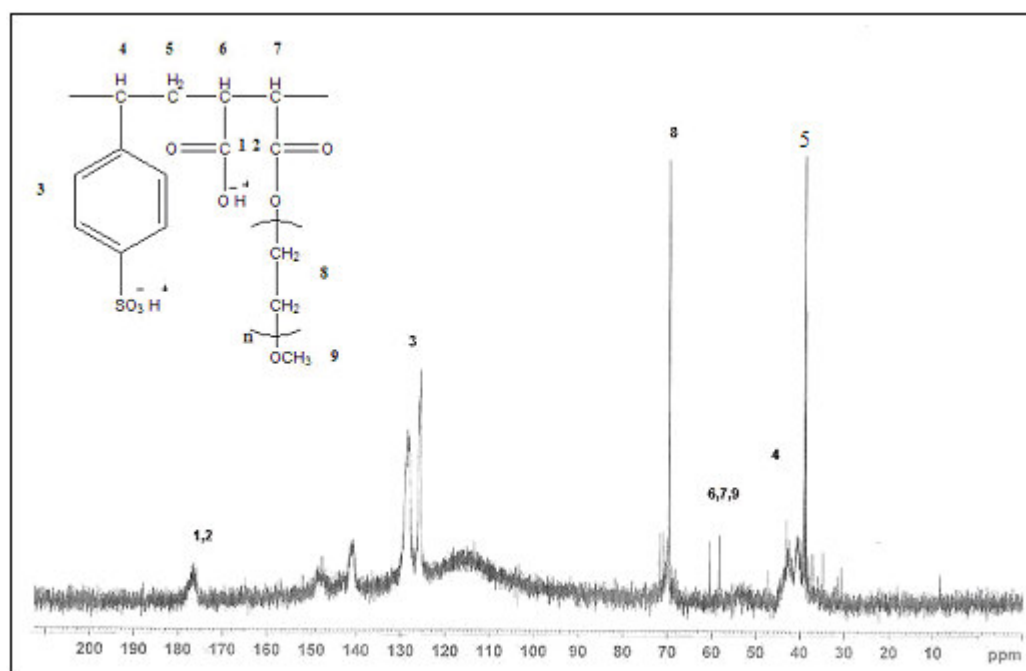


Figure 3.8 ¹³C NMR spectrum of A33

3.1.2.3. ^1H and ^{13}C NMR Characterization of B55

Fig. 3.9 and 3.10 shows ^1H and ^{13}C NMR spectra of B55. The chemical shifts of B55 are as follows: δ 7.6 (6H) (1), 3.71 (4H) (2), 2.9 (3H) (3) in ^1H NMR spectrum and δ 165 (1C,2C), 140-117 (3Ar), 40 (4C), 31 (5C), 60 (6C), 58 (7C), 69 (8C), 66 (9C) in ^{13}C NMR spectrum.

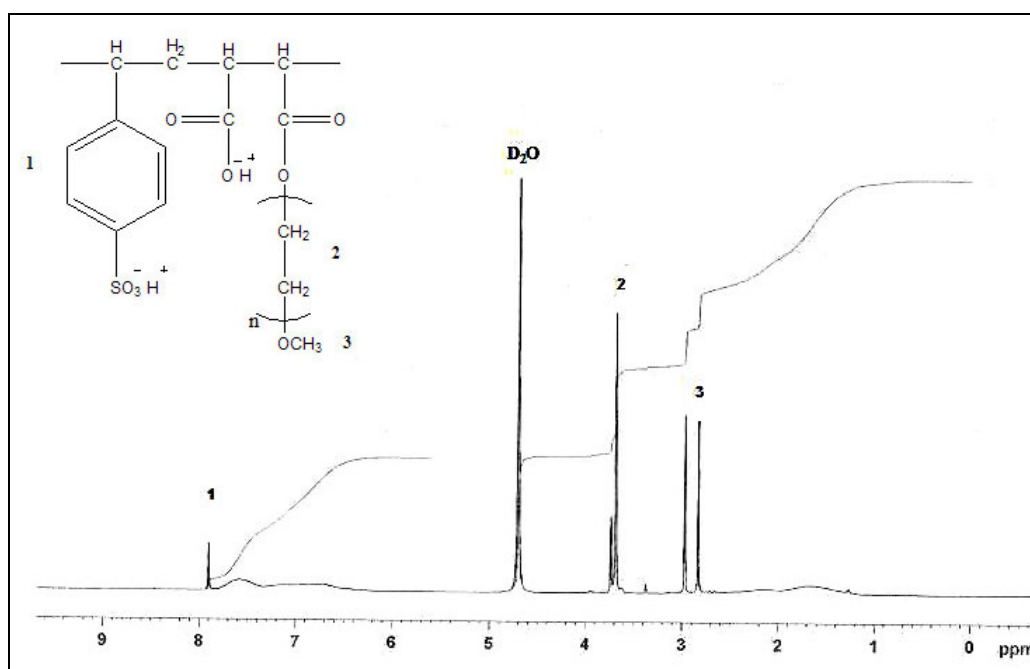


Figure 3.9 ^1H NMR spectrum of B55

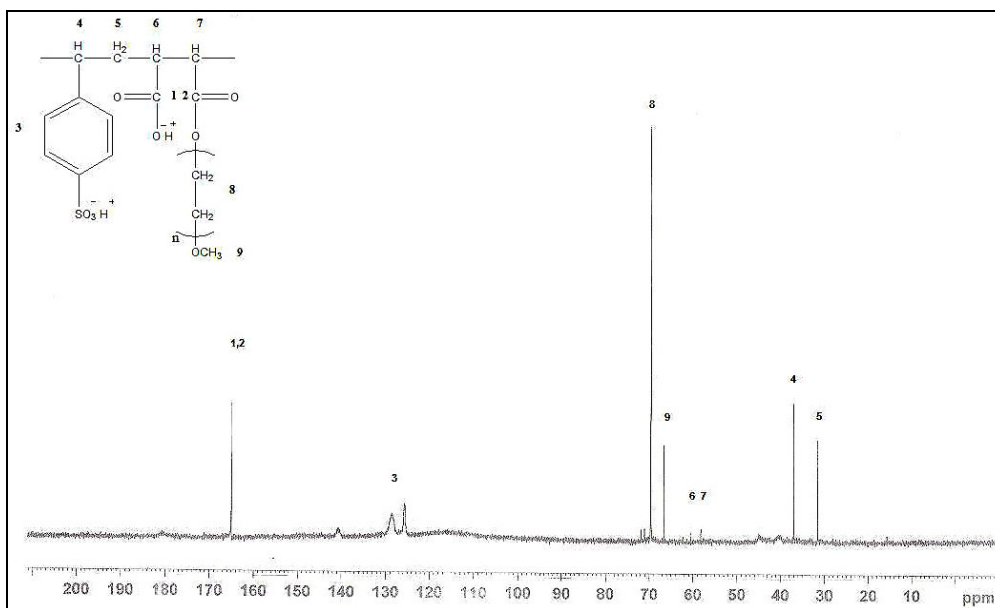


Figure 3.10 ^{13}C NMR spectrum of B55

3.2. Dilute Solution Viscosity Results

Dilute solution viscosimetry measurements are performed in order to study the effect of molecular weight on mini slump tests. Molecular weight is an important parameter which affects fluidity. Since the samples show polyelectrolyte behaviour, their intrinsic viscosities cannot be determined. So η_{sp}/C vs. C plots give some comparative information about the sizes of the molecules.

3.2.1. Dilute Solution Viscosity of SSAMA

In Fig. 3.11 the η_{sp}/C vs. C results for SSAMA is illustrated. It is seen that SSAMA is a polyelectrolyte because of its high ionizable groups containing

sodium salts. The viscosity increases markedly as polymer concentration decreases with consequent increase in degree of ionization of the polymer.

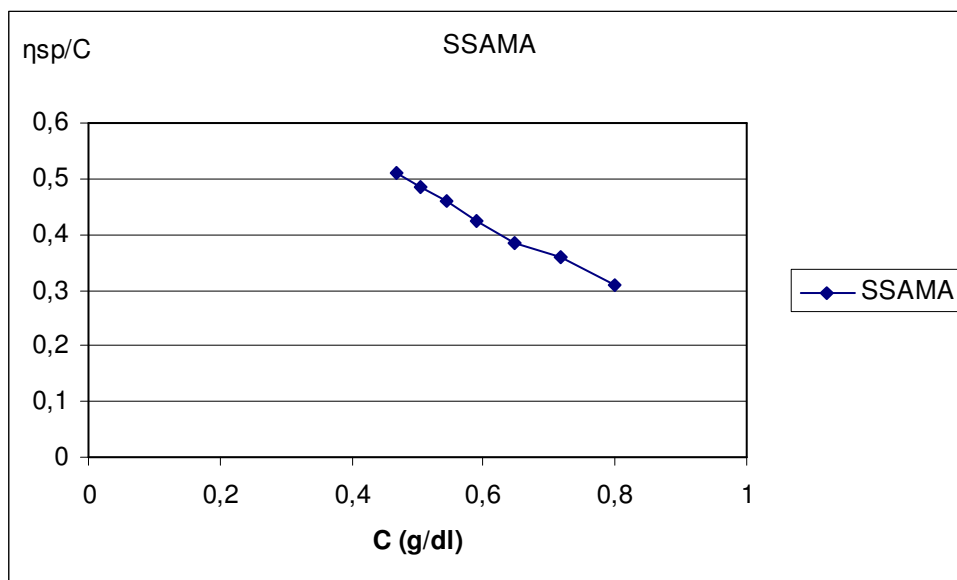


Figure 3.11 The plot of η_{sp}/C vs. C for SSAMA

3.2.2. Dilute Solution Viscosity of A32 and A41

In Fig. 3.12 the relationship of η_{sp}/C vs. C with different PEG compositions of the copolymers is illustrated. It is seen that the viscosity average molecular weight of A32 and A41 is slightly higher than the viscosity average molecular weight of SSAMA at 0.8 g/dl concentration. Logically it is expected that PEG grafted copolymers must have higher molecular weights than the molecular weight of SSAMA.

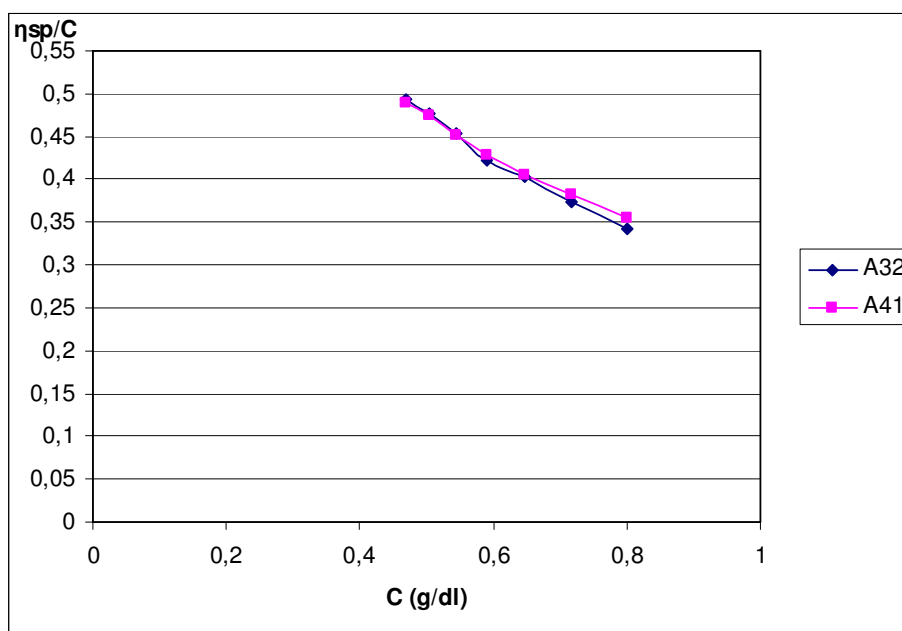


Figure 3.12 The plot of η_{sp}/C vs. C for A32 and A41

Additionally, the grafted copolymers exhibit polyelectrolytic behaviour, i.e. increase in viscosity with decrease in polyelectrolyte concentration. Both the intrinsic viscosity of the grafted copolymers exhibits the same trend line.

3.2.3. Dilute Solution Viscosity of B64 and B82

In Fig. 3.13 the η_{sp}/C vs. C results of PEG1100 grafted SSAMA are illustrated. The polyelectrolytic behaviour of B82 exhibits excellent trend line according to other copolymers. As the process continues with further dilution for both of the copolymers, the expansive forces increases thus the intrinsic viscosity increases. The molecular weight of both copolymers is higher than the molecular weight of SSAMA as expected.

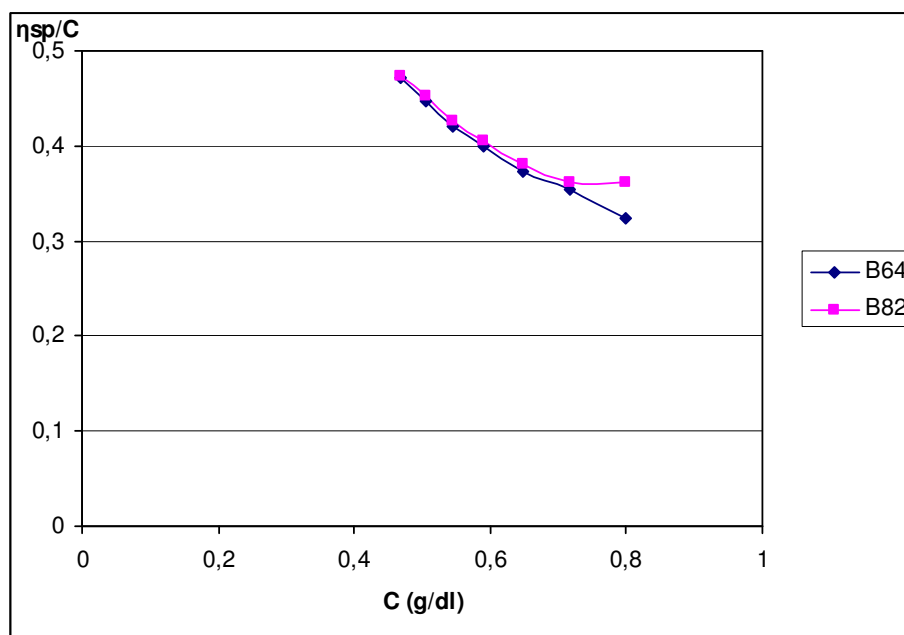


Figure 3.13 The plot of η_{sp}/C vs. C for B64 and B82

3.3. Zeta Potential Results

In Fig. 3.14 the zeta potential values for SSAMA and its PEG grafted samples with different compositions and molecular weights and different Li^+ salts of SSAMA in water are given. It is seen that the zeta potentials for the slurries containing SSAMA and its derivatives are highly negative. The magnitude of the zeta potential gives an indication of the potential stability of the colloidal system. If all the particles in suspension have a large negative or positive zeta potential they will tend to repel each other and there will be no tendency for the particles to come together. However, if the particles have low zeta potential values then there will be no force to prevent the particles coming together and flocculation takes place. The general dividing line between stable and unstable suspensions is generally taken at either +30 or -30 mV. Particles with zeta potentials more positive than +30 mV or more negative than -30 mV are normally considered stable [20].

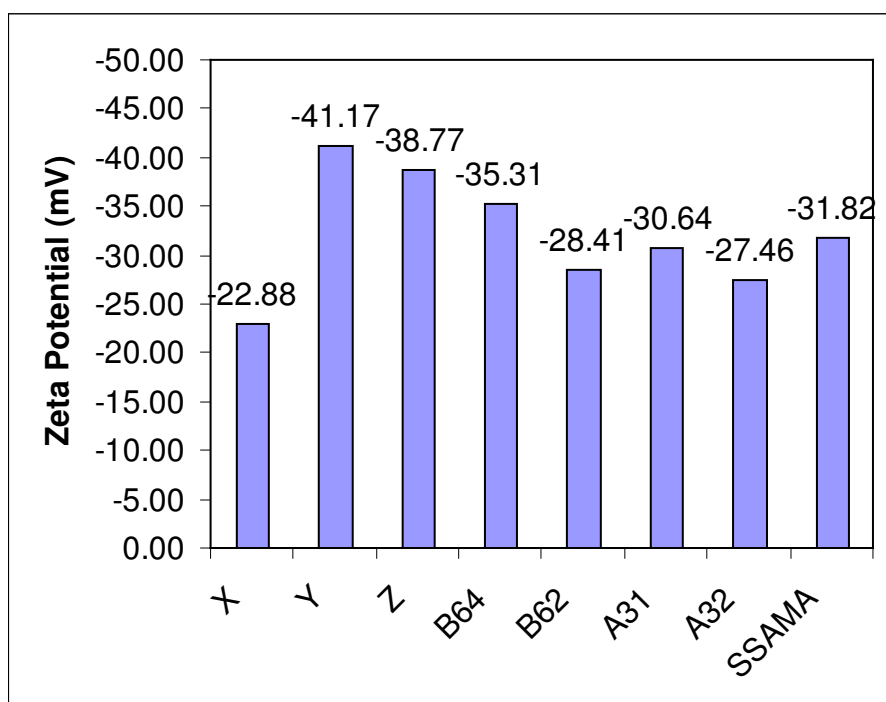


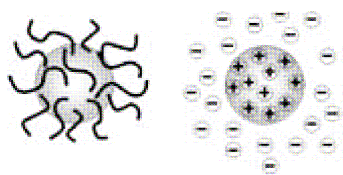
Figure 3.14 Effects of superplasticizers on the zeta potential of cement particle surface (X: LiCl, Y: Li_2CO_3 , Z: Li_2SO_4)

According to this knowledge the zeta potentials of SSAMA containing LiCl salts in 1:1 composition (-22.88 mV) and B62 (-28.41 mV), and A32 (-27.46 mV) are considered to be unstable. The zeta potential of SSAMA containing Li_2CO_3 (-41.17 mV) and Li_2SO_4 (-38.77 mV) salts, A31 (-30.64 mV) and B64 (-35.31 mV) are more negative than -30 mV, so they are stable. Also the zeta potential of SSAMA is -31.82 mV that indicates stability.

The thickness of the electrical double layer (κ^{-1}) depends upon the concentration of the ions in solution and can be calculated from the ionic strength of the medium. The higher the ionic strength, the more compressed the double layer becomes. The valency of the ions will also influence double layer thickness [20]. The divalent ions i.e. CO_3^{2-} and SO_4^{2-} will compress the double layer to a greater extent in comparison with a monovalent ion such as

Cl^{-1} . Thus the zeta potential of these ions of salts is higher than the ions of LiCl salt.

Superplasticizers are adsorbed on the surface of cement particles, which deflocculates. Basically there are two types of dispersion mechanisms: Electrostatic repulsion and steric hindrance [26]. These two fundamental mechanisms maintain the stability of the colloidal system. (Fig. 3.15) Uchikawa et al. reported that sulfonated superplasticizers give rise to a higher zeta potentials than PEG grafted polycarboxylate superplasticizers [15]. According to the studies of Björnstrom et al. sulfonated superplasticizers induced a negative charge on cement particles dispersing them by electrostatic repulsion, whereas with the PEG grafted polycarboxylate based polymers the dispersion mechanism is mainly controlled by steric hindrance [14]. Anderson et al. have reported that the sulfonated superplasticizers with largest molecular weights give the largest negative zeta potentials and therefore as having higher dispersing capability. The absence of long side chains provide the smaller sulfonated polymers with a higher charge density than the heavier PEG grafted polycarboxylate type polymer, therefore the electrostatic repulsion is more pronounced [14].



Steric stabilization Electrostatic stabilization

Figure 3.15 Steric and electrostatic stabilization mechanisms of colloidal dispersions

SSAMA is a sulfonated polycarboxylate superplasticizer. The molecular weight of this copolymer is 20000 g/mol in 3:1 (styrene/maleic acid unit) composition. These PEG grafted copolymers of SSAMA have high molecular weight which is made up of a backbone containing carboxylic groups, sulfonated groups and polyoxyethylene side chains. The long side chains contribute to the role of steric hindrance and sulfonated groups contribute to electrostatic repulsion. In the composition of SSAMA; the sulfonated styrene units are greater than maleic acid units, therefore it may be concluded that the dispersion mechanism of SSAMA is mainly controlled by electrostatic repulsion. PEG grafted SSAMA copolymers have a higher charge density and therefore the zeta potential of these superplasticizers are very negative.

3.4. Mini Slump Test

The relative slump test results demonstrate the effect of PEG grafting with different molecular weights and the different compositions and the effect of LiCl, Li₂CO₃ and Li₂SO₄ salts with various compositions on the fluidity of cement paste.

3.4.1. Mini Slump Test Results for PEG2000 Grafted SSAMA

Figure 3.16 represents the relative slump of PEG2000 grafted copolymers. It is clear that the polymer samples with different compositions of PEG contents exhibit different fluidity enhancing capacities. As the degree of grafting increases, the fluidity increases, too. The maximum fluidity achieved for the sample A33. SSAMA copolymer with a higher PEG content exhibits better

dispersing capability compared to lower PEG compositions. As the copolymer contains more comb-type side chains, the steric hindrance becomes more effective and the fluidity of the cement paste is increased.

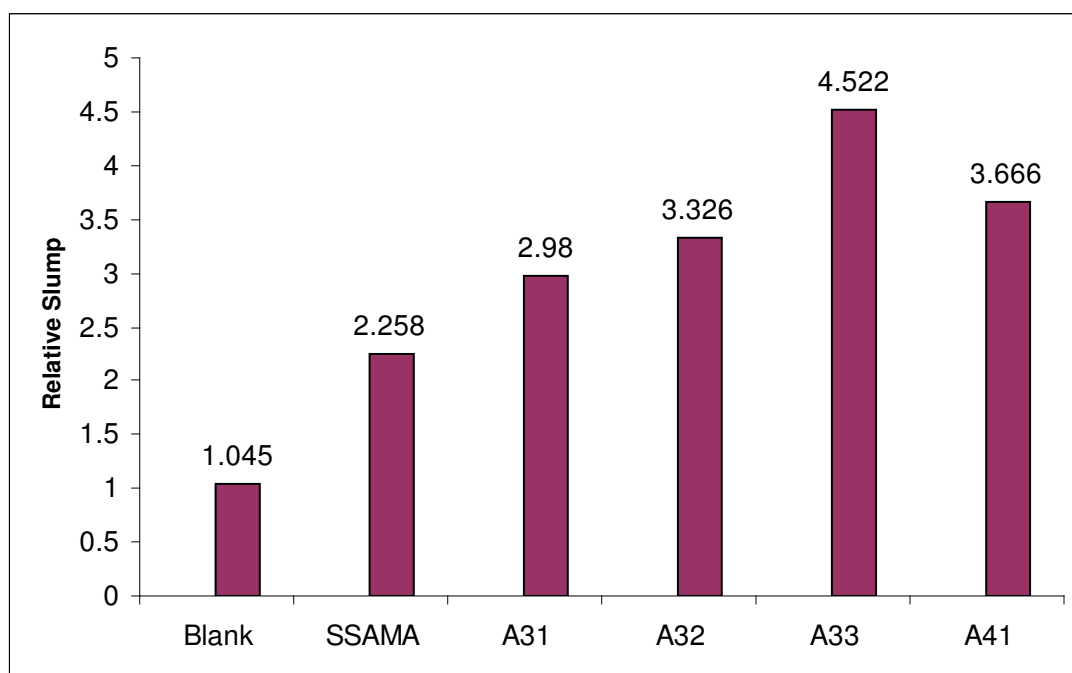


Figure 3.16 Relative slump of PEG2000 grafted SSAMA

3.4.2. Mini Slump Test Results for PEG1100 Grafted SSAMA

Fig. 3.17 shows the relative slump of PEG1100 grafted copolymers. In this experiment the effect of chain length to the fluidity is studied. PEG side chains with largest molecular weight also have greater chain length. Therefore the overall flow values of these grafted copolymers are less than the PEG2000 grafted copolymers.

The highest fluidity is expected for B55* because of the highest PEG content. But the maximum flow value is observed for B64. As it is seen in the figure the flow values shows a maximum and when overall PEG content is further increased, it starts decreasing. If the fluidity results of PEG2000 and PEG1100 grafted copolymers are compared, it is understood that the presence of long side chains gives better dispersing ability.

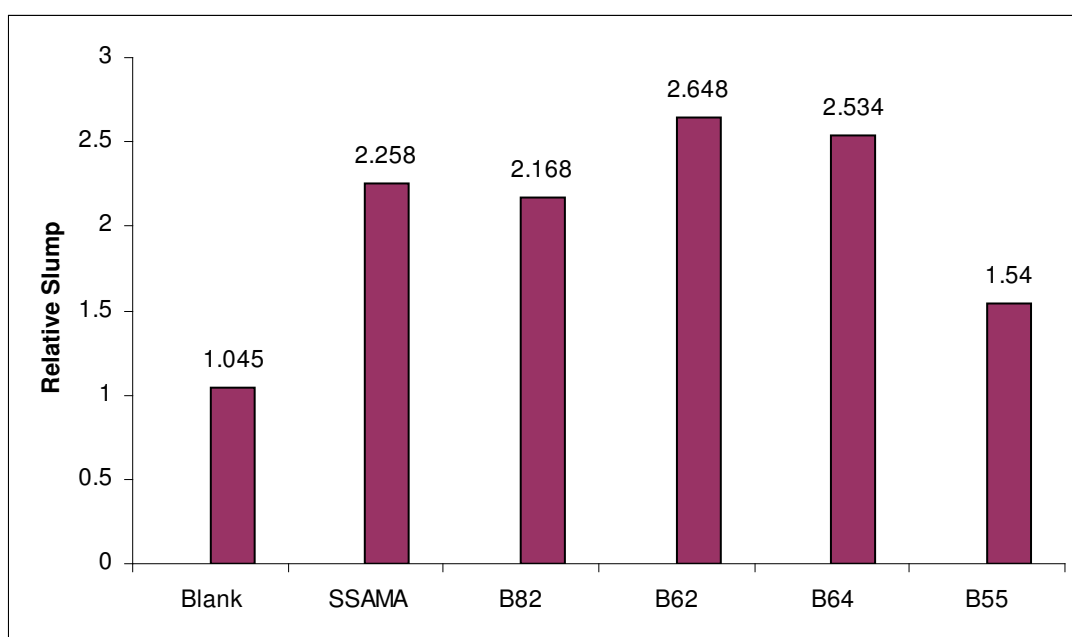


Figure 3.17 Relative slump of PEG1100 grafted SSAMA

* The mini-slump flow test is done by different production of Portland cement (CEM I 42.5)

3.4.3. Mini Slump Test Results for Li salts of SSAMA

In this experiment the effect of change of ionic medium is studied. In Fig. 3.18 the relative flow ratios of various Li^+ salts of SSAMA are illustrated. The mixture of LiCl : SSAMA (1:1 mol ratio) exhibits the relative slump. It is seen that as the amount of the salts increases, relative slump also increases but the excess amount of the salts except Li_2SO_4 decreases the relative slump.

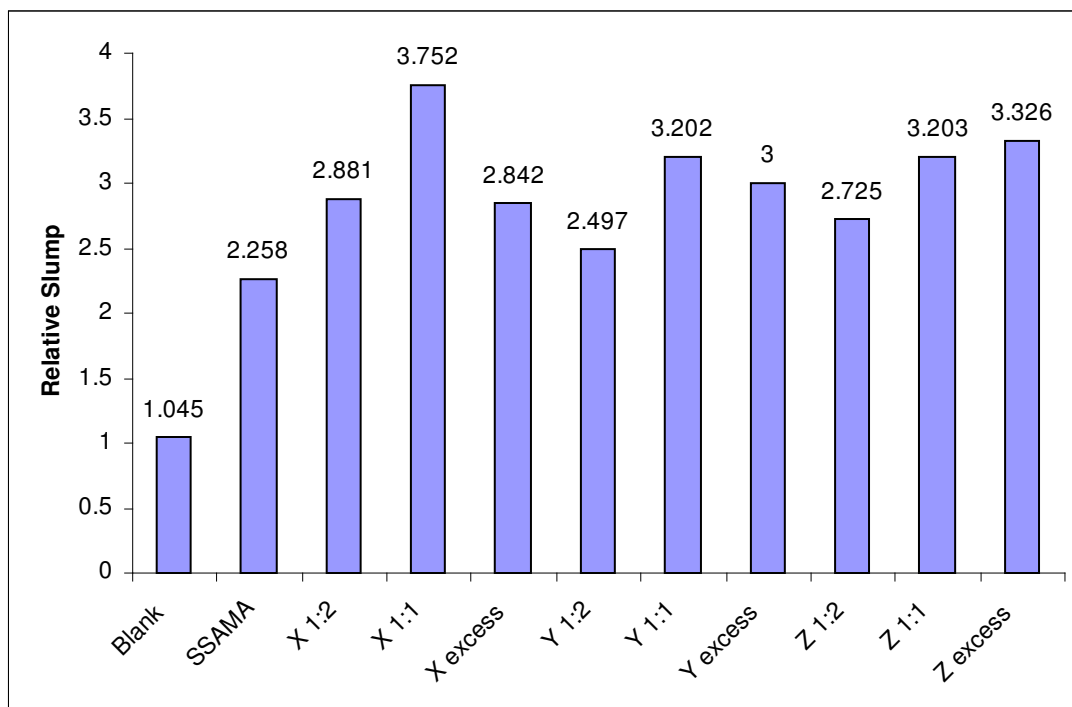


Figure 3.18 The relative slump of SSAMA containing various Li salts with different compositions (X= LiCl : SSAMA, Y= Li_2CO_3 : SSAMA, Z= Li_2SO_4 : SSAMA)

In Fig. 3.19 the ionic strength of Li salt solutions are plotted against relative slump. The ionic strength of the solution containing ions is calculated by Eq. (3.1)

$$I = \frac{1}{2} \sum (c_i \times z_i^2) \quad (3.1)$$

where i is the kind of ion, z_i is the the charge number of ion i , and c_i is the molar concentration of ion i [27].

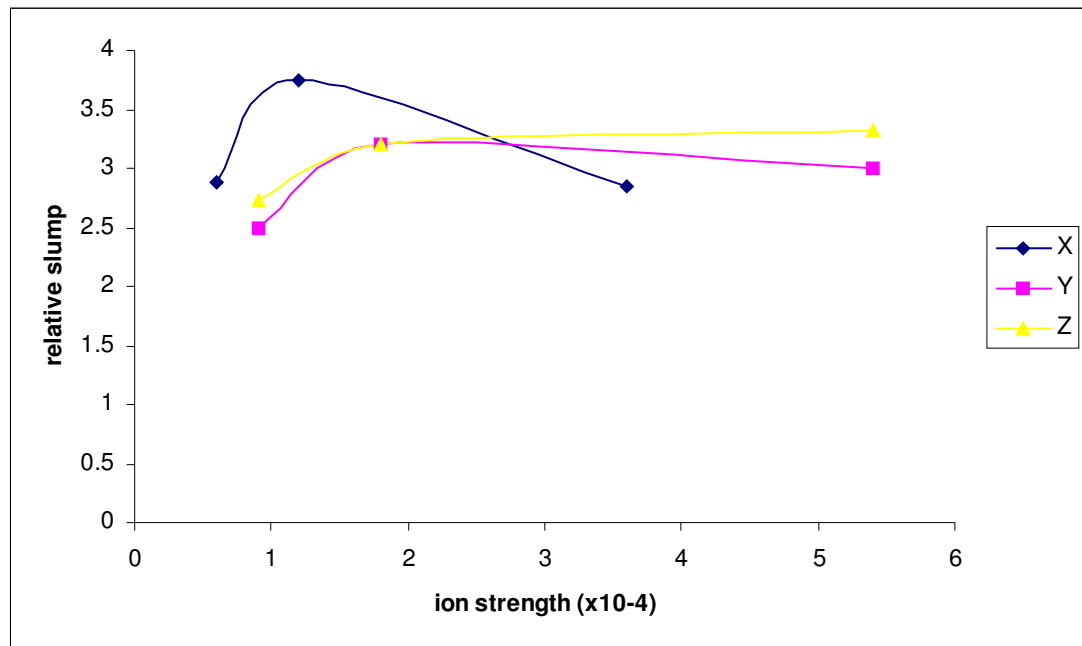


Figure 3.19 The effects of ion strength on paste fluidity (X: LiCl, Y: Li₂CO₃, Z: Li₂SO₄ solution of SSAMA)

In the figure above, by the addition of LiCl and Li₂CO₃ salts, the fluidity increases up to a constant value and decreases when the amount of the salt is excess that depends on the anion type. The optimum composition of these

salts that show the highest fluidity is 1:1 (Li salt : SSAMA) mol ratio. Yamada et al. considered that the main chain expands in aqueous solutions by the dissociation of the carboxylic group because the dissociation generates the electrostatic repulsive force between carboxylic groups. The dissociated state is expected to change depending on the ionic strength. In higher ionic solutions, since the dissociation is less, the repulsive force between the carboxylic groups is weaker [27]. Due to these weak repulsive forces, the fluidity of LiCl and Li₂CO₃ salts decreases when the ionic strength is high. However, by the addition of Li₂SO₄ salt, the fluidity increases; although the ionic strengths of Li₂SO₄ and Li₂CO₃ are the same.

3.5. Mechanical Strength Test Results

3.5.1. Flexural Strength Test Results

Maximum flexural stresses experienced by the mortar samples at their moment of rupture are given in Table 3.1.

Table 3.1 Maximum flexural stresses experienced by the mortar samples

		Force (kgf)			Force (kgf)
A	Sample 1	214	E	Sample 1	240
	Sample 2	212		Sample 2	246
	Sample 3	198		Sample 3	240
B	Sample 1	220	F	Sample 1	260
	Sample 2	250		Sample 2	262
	Sample 3	234		Sample 3	240
C	Sample 1	250	G	Sample 1	240
	Sample 2	246		Sample 2	252
	Sample 3	256		Sample 3	245
D	Sample 1	254			
	Sample 2	250			
	Sample 3	220			

Samples illustrated with the letters in the Table 3.1 are defined as:

- A: The blank mortar (with no admixture)
- B: SSAMA
- C: A33
- D: B55
- E: Li_2CO_3 salt of SSAMA (1:1 composition)
- F: LiCl salt of SSAMA (1:1 composition)
- G: Li_2SO_4 salt of SSAMA (1:1 composition)

The stress data obtained from the flexural strength test is inserted into the equation 2.11 and the units are converted according to N/mm^2 , the average flexural strength results of the mortar samples in kgf/cm^2 and N/mm^2 are represented in Table 3.2.

Table 3.2 Flexural strengths of mortar samples

	A	B	C	D	E	F	G
kgf/cm ²	58.5	66.0	70.5	67.875	68.063	71.438	69.094
N/mm ²	5.733	6.468	6.909	6.652	6.670	7.001	6.771
std.dev.	2.45	4.222	1.416	5.227	0.974	3.422	1.695

The discussion for the flexural strength results and the compressive strength results will be done together.

3.5.2. Compressive Strength Test Results

Maximum compressive stresses experienced by the mortar samples at the moment at which the samples are crashed are given in Table 3.3.

Table 3.3 Maximum compressive stresses experienced by the mortar samples

		Force (kgf)			Force (kgf)
A	Sample 1	5105	E	Sample 1	6410
	Sample 2	5140		Sample 2	6605
	Sample 3	5535		Sample 3	3563
B	Sample 1	6385	F	Sample 1	6230
	Sample 2	6340		Sample 2	6270
	Sample 3	6095		Sample 3	6175
C	Sample 1	6485	G	Sample 1	5760
	Sample 2	6490		Sample 2	5795
	Sample 3	6640		Sample 3	5995
D	Sample 1	5465			
	Sample 2	6445			
	Sample 3	6560			

The average compressive strength data calculated in kgf/cm^2 and N/mm^2 from equation 2.12 are given in Table 3.4.

Table 3.4 Compressive strengths of the mortar samples

	A	B	C	D	E	F	G
kgf/cm^2	328.83	392.17	408.67	385	405.67	389.17	365.67
N/mm^2	32.225	38.433	40.049	37.73	39.756	38.139	35.836
std.dev.	9.928	10.347	35.179	13.688	11.308	7.359	11.639

The water content of all mortar samples are the same, thus their mechanical properties are expected to be relatively higher than the blank mortar. Since the copolymers which are water reducing agents, will reduce the water content of the concrete, their mechanical strengths are expected to improve to a noticeable values [28].

The sample C which is defined as A33, shows maximum flexural strength and maximum compressive strength compared to SSAMA (sample B) and B55 (sample D) and also has a higher fluidity. The PEG content is higher in A33 so the molecular weight of the copolymer is higher than the other copolymers, thus it gives a rise to higher fluidity, higher flexural strength and higher compressive strength. The long side chains of A33 interact with cement particles better than the other samples.

LiCl salt of SSAMA which is labeled as the sample F shows maximum flexural strength and Li_2CO_3 salt of SSAMA which is labeled as the sample E shows maximum compressive strength. LiCl salt of SSAMA in 1:1 composition also gives higher fluidity in mini slump tests. It is understood that the presence of Li salts in water solution of SSAMA, increases the mechanical properties of mortars.

CHAPTER 4

CONCLUSION

In this study poly (4-styrenesulfonic acid-co-maleic acid) sodium salt and its PEG grafted copolymers with various weight compositions and the solutions of various Li salts of SSAMA used as the water reducing agents in cement. According to the results of these analyses, the following conclusions are obtained:

- 1) FTIR spectroscopy is an important experimental technique to support the successful grafting of PEG to SSAMA copolymer. The stretching band of C=O at around 1700 cm^{-1} and the sharp peak at 1496.28 cm^{-1} is related to C-H bending of CH_2 groups in the side chain revealed the successful grafting of PEG.
- 2) According to the NMR spectra of A33 and B55 the intensive peaks at approximately 3.60 and 2.65 ppm belong to the protons of CH_2 groups and the protons of methoxy groups in the side chains respectively.
- 3) The dilute solution viscosity measurements of PEG grafted copolymers having different molecular weights and compositions were determined in water at 25°C . It was observed that grafting of PEG to SSAMA copolymer relatively increased the molecular weight and this result was also observed for the values of fluidity of these copolymers.

- 4) Zeta potential results give an indication about the potential stability of the colloidal systems. According to the studies of Uchikawa and Björnstrom et al. sulfonated superplasticizers give higher zeta potentials than PEG grafted polycarboxylate superplasticizers and the dispersion is controlled by electrostatic repulsion. The dispersion mechanism of SSAMA is mainly controlled by electrostatic repulsion because of the ratio of sulfonated styrene groups to carboxylic groups is 3:1. So the zeta potential of SSAMA (-31.82 mV) confirmed the dispersion mechanism. The anion charge of Li salts affects the zeta potential of the slurries. The divalent anions of Li salts compress the double layer therefore it increases the zeta potential.
- 5) The maximum flow value is observed for A33, which has the highest amount of PEG. The molecular weight of PEG affects the side chain length as a result fluidity of the cement paste is also increased. The addition of Li^+ salts improved the fluidity of cement paste. The effect of LiCl salt solution, which has 1:1 composition shows the highest fluidity. Excess amounts of LiCl and Li_2CO_3 salts decreases the fluidity except the Li_2SO_4 salt of SSAMA.
- 6) The mechanical properties of A33 show maximum flexural strength and maximum compressive strength compared to blank mortar and SSAMA. The high molecular weight of the grafted copolymer and long side chains affect the interactions with cement particles and shows better dispersing capability.
- 7) The presence of the salts in water solution of SSAMA, increases the mechanical properties of mortars. LiCl salt of SSAMA, which is labeled as the sample F shows maximum flexural strength and Li_2CO_3 salt of SSAMA, which is labeled as the sample E shows maximum compressive strength.

REFERENCES

- [1] Ramachandran V.S., *Handbook of Analytical Techniques in Concrete Science and Technology, Principles, Techniques and Applications*, Noyes Publications, U.S.A., 2001
- [2] Brewer J, Concrete, Scientific principles. Last accessed date February 14, 2008 from <http://matse1.mse.uiuc.edu/concrete/concrete.html>
- [3] Yoshioka K., Tazawa E., Kawai K., Enohata T., Adsorption Characteristics of Superplasticizers on Cement Component Minerals, *Cem. Concr. Res.* 32 (2002) 1507-1513
- [4] Jolicoeur C., Simard M.A., Chemical Admixture-Cement Interactions: Phenomenology and Physicochemical Concepts, *Cem. Concr. Comp.* 20 (1998) 87-101
- [5] Collepardi M., Admixtures Used to Enhance Placing Characteristics of Concrete, *Cem. Concr. Comp.* 20 (1998) 103-112
- [6] Hover K.C., Concrete Mixture Proportioning with Water-Reducing Admixtures to Enhance Durability, *Cem. Concr. Comp.* 20 (1998) 113-119
- [7] Ohama Y., *Handbook of Polymer Modified Concrete and Mortars Properties and Process Technology*, Noyes Publications, U.S.A., 1995
- [8] Rixom R., Mailvaganam N., *Chemical Admixtures for Concrete*, E. & F.N., London, 1999

[9] Neville A.M., *Properties of Concrete*, Pearson Prentice Hall, London, 2002

[10] Ramachandran V.S., *Concrete Admixtures Handbook, Properties, Science and Technology*, Noyes Publications, U.S.A., 1995

[11] Rabbii A., Synthesis of Water Soluble Highly Sulphonated Melamine-Formaldehyde Resin as an Effective Superplasticizer in Concrete, Iran. Polym. J. 10, 3 (2001) 157-163

[12] Puertas K., Santos H., Palacios M., Ramirez-Martinez S., Polycarboxylate Superplasticizer Admixtures: Effect on Hydration, Microstructure and Rheological Behaviour in Cement Pastes, Adv. Cem. Res. 17, 2 (2005) 77-89

[13] Yamada K., Takahashi T., Hanehara S., Matsuhisa M., Effects of the Chemical Structure on the Properties of Polycarboxylate Type Superplasticizer, Cem. Concr. Res. 30 (2000) 197-207

[14] Björnstrom J., Chandra S., Effects of Superplasticizers on the Rheological Properties of Cements, Materials and Struct. 36 (2003) 685-892

[15] Uchikawa H., Hanehara S., Sawaki D., The Role of Steric Repulsive Force in the Dispersion of Cement Particles in Fresh Paste Prepared with Organic Admixture, Cem. Concr. Res. 27, 1 (1997) 37-50

[16] Nawa T., Effect of Chemical Structure on Steric Stabilization of Polycarboxylate based Copolymer, Journ. Adv. Concr. Tech. 4, 2 (2006) 225-232

[17] Ohta A., Sugiyama T., Tanaka Y., Fluidizing Mechanism and Application of Polycarboxylate based Superplasticizers Containing Polyethylene Oxide Graft Chains, American Concrete Institute Special Publication SP-173 (1997) 359-378

[18] Andersen P.J., Roy D.M., The Effects of Adsorption of Superplasticizers on the Surface of Cement, Cem. Concr. Res. 17, 5 (1987) 805-813

[19]] Flatt R.J., Houst Y.F., Oesch R., Bowen P., Hofmann H., Widmer J., Sulser U., Maeder U., Bürge T.A., Analysis of Superplasticizers used in Concrete, La Chromatographie Liquide HPLC 26, 2 (1998) M28-35

[20] Malvern Instruments Ltd., Zeta Potential. Last access date February 1, 2008 from <http://www.malvern.com/labeng/products/iwtm/zetapotential.htm>

[21] Şahmaran M., Christianto H.A., Yaman İ.Ö., The Effect of Chemical Admixtures and Mineral Additives on the Properties of Self-Compacting Mortars, Cem. Concr. Comp. 28 (2006) 432-440

[22] Tuzcu G., 2-Acrylamido-2-Methyl-1-Propanesulfonic Acid-methacrylic Acid Copolymer and its Polyethylene Glycol Methyl Ether Derivatives as Superplasticizers in Concrete (2008) Ankara: METU

[23] Erdoğan T.Y., Materials of Construction (2002) Ankara: METU

[24] Kumar A., Lahiri S.S., Singh H., Development of PEGDMA: MAA based Hydrogel Microparticles for Oral Insulin Delivery, Int. Journ. Pharm. 323 (2006) 117-124

[25] Ye Y.S., Huang H.L., Hsu K.C., A Water Soluble Acrylate/Sulfonate Copolymer. I. Its Synthesis and Dispersing Ability on Cement, Journ. App. Polym. Sci. 100 (2006) 2490-2496

[26] Chandra S., Björnström J., Influence of Superplasticizer Type and Dosage on the Slump Loss of Portland Cement Mortars-Part I, Cem. Concr. Res. 32, 10 (2002) 1605-1611 (7)

[27] Yamada K., Ogawa S., Hanehara S., Controlling of the Adsorption and Dispersing Force of Polycarboxylate Type Superplasticizer by Sulfate Ion Concentration in Aqueous Phase, Cem. Concr. Res. 31 (2001) 375-383

[28] Akovali G., Polymers in Construction, Shropshire: Rapra Technology Limited. (2005)

APPENDIX A

FTIR SPECTRA OF THE GRAFTED COPOLYMERS

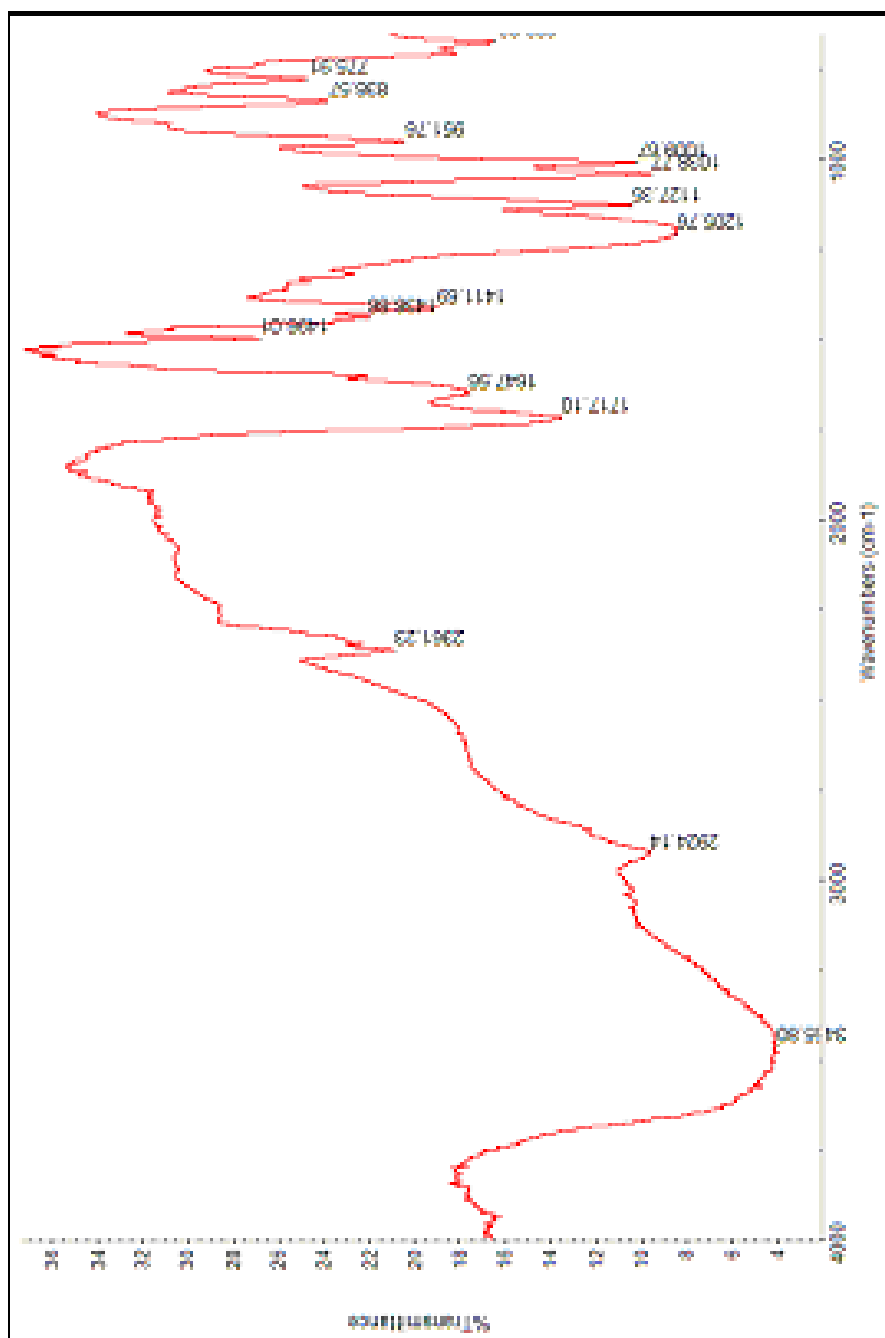


Figure A. 1 FTIR spectrum of A32

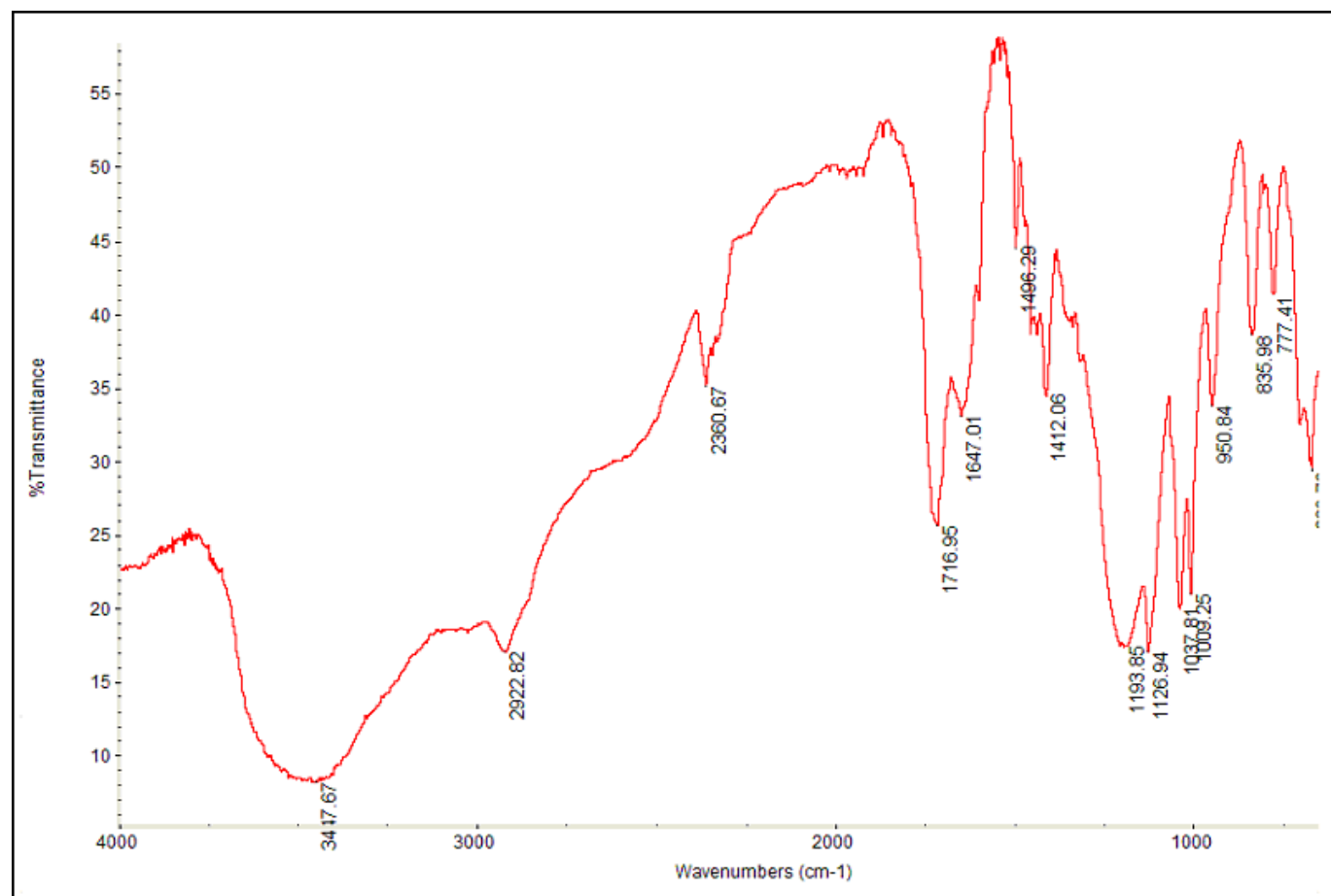


Figure A. 2 FTIR spectrum of A33

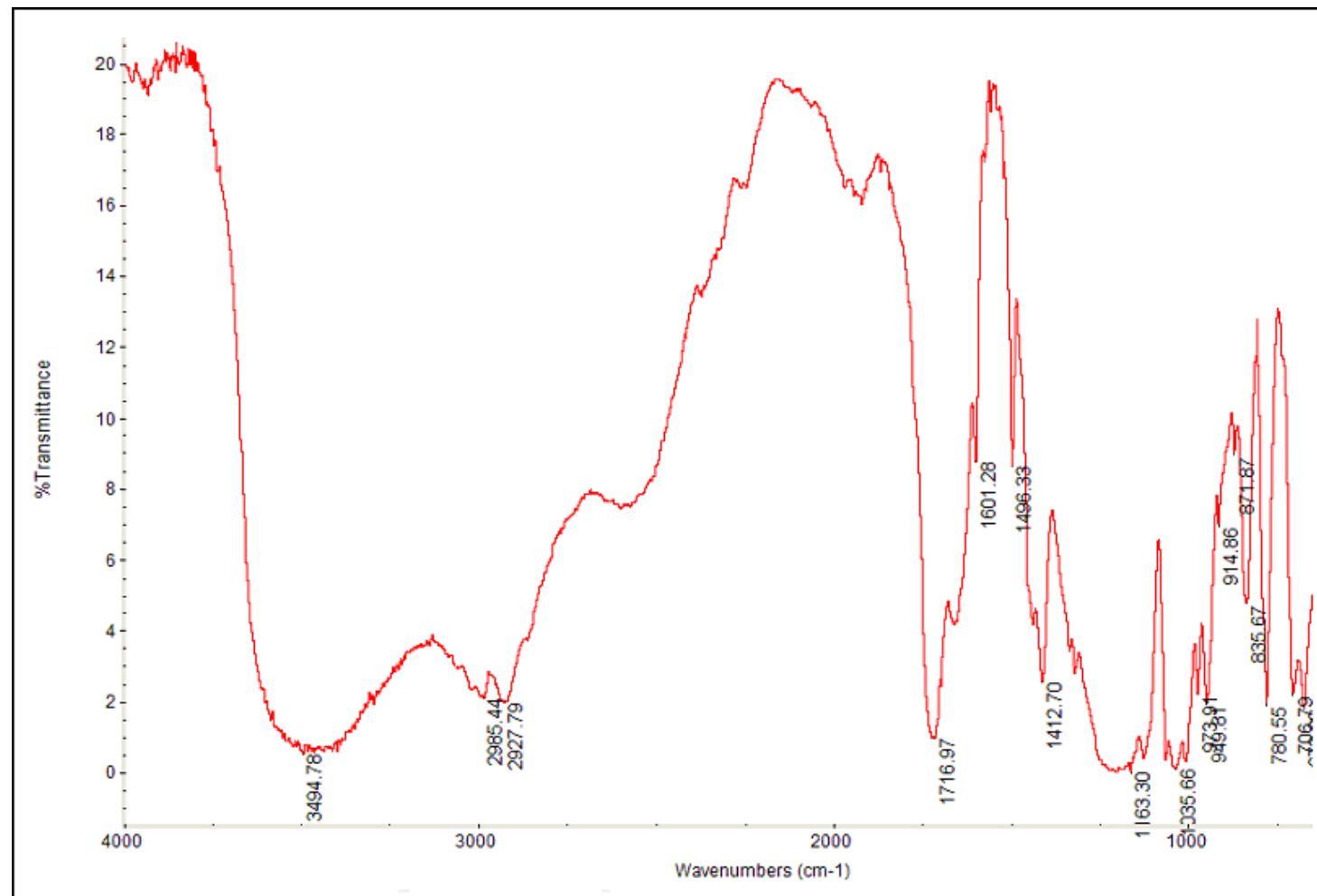


Figure A. 3 FTIR spectrum of A41

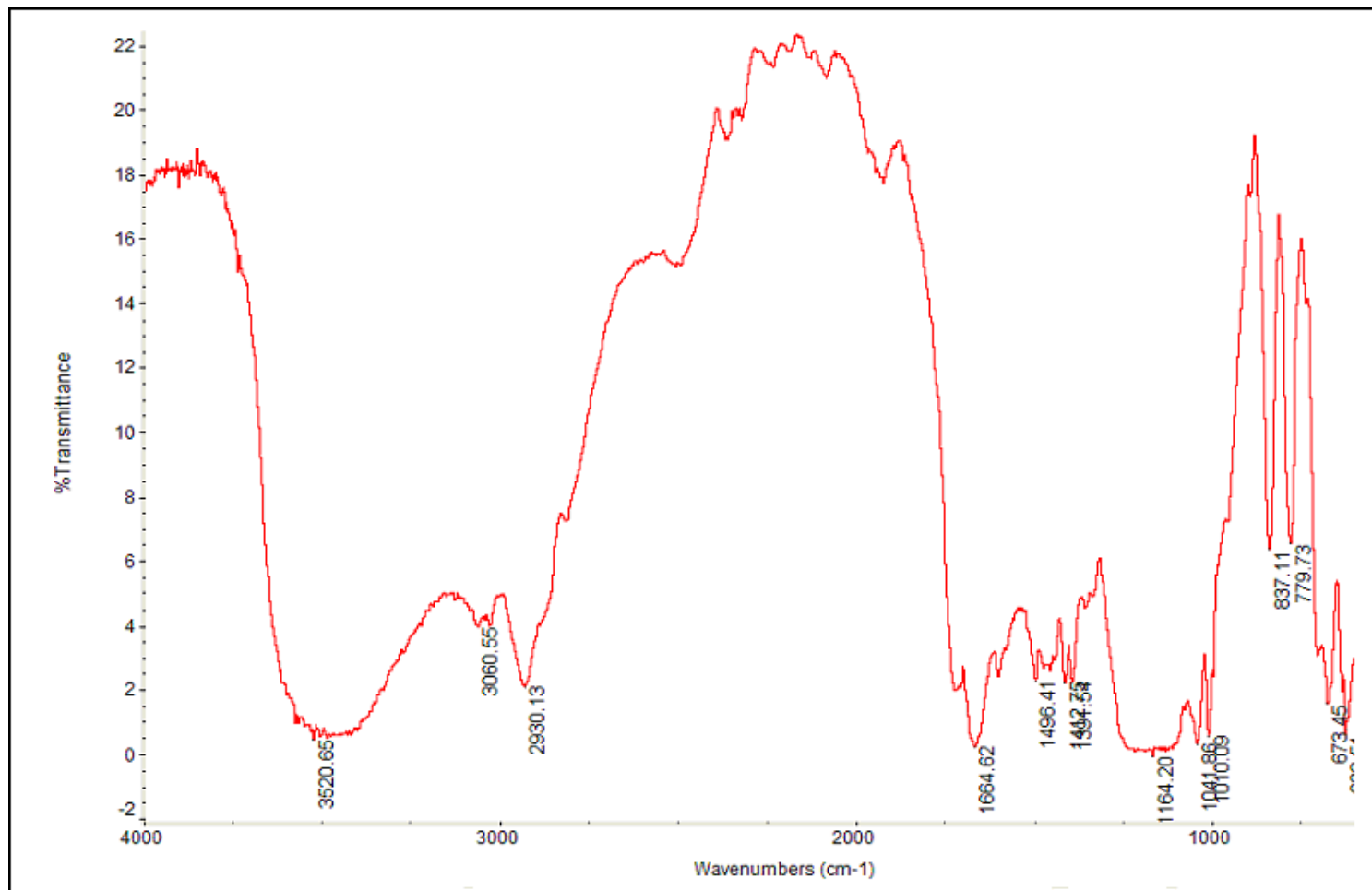


Figure A. 4 FTIR spectrum of B82

